Application of Response Surface Methodology and Artificial Neural Network for Optimizing Phosphate Removal from Lagoon Wastewater

By

Aidin Khordadi

Master of Science

Department of Civil Engineering
University of Manitoba
Winnipeg, Manitoba, Canada

Abstract

Lagoons are primary wastewater treatment methods used in rural municipalities and small communities in Canada. This study aimed to optimize phosphate removal and reduce generated sludge in lagoon wastewater treatment under varying operational parameters. Two series of bench-scale experiments were conducted to evaluate phosphate removal and sludge production using aluminum sulphate and ferric chloride as coagulants, and cationic polymers as coagulant aids. Two models were developed to predict optimal conditions for phosphate removal and sludge production.

Response Surface Methodology (RSM) with optimal design was employed to assess the impact of pH, temperature, coagulant dosage and type, and flocculant type and dosage on the responses. Subsequently, a feedforward multilayer Artificial Neural Network (ANN) model was developed based on RSM inputs, along with floc perimeter and area, to forecast final phosphate levels in effluent and the amount of generated sludge.

The results revealed that polymers with 40% cationic charge and higher molecular weight were more efficient compared to polymers with higher charge and lower molecular weights. Additionally, the R-squared (R^2) values for the RSM models were 0.9264 and 0.9194 for phosphate removal and sludge production, respectively. The corresponding R^2 values for the ANN models were 0.7994 and 0.7965, indicating good predictive performance.

Acknowledgement

I would like to deeply thank my supervisor, Dr. Qiuyan Yuan, for your invaluable mentorship, encouragement, and insightful feedback throughout this research. Your expertise and guidance have been instrumental in shaping this thesis and my academic growth.

I am also grateful to our diligent lab manager, Dr. Victor Wei, whose assistance with experimental setups and technical support greatly facilitated the progress of my research. Your dedication and expertise have been indispensable.

I owe a special debt of gratitude to my wife, Nasim, for her unwavering love, encouragement, and patience during this demanding period. Your support and understanding have sustained me through the challenges of my study. Nasim, you have been always supportive of the decisions that I have made. I love you so much.

Lastly, I would like to extend my heartfelt thanks to my friends in our research group for their encouragement, moral support, and occasional distractions that provided much-needed breaks. Your camaraderie has made this journey memorable and enjoyable. I am truly fortunate to have had such wonderful individuals in my corner throughout this thesis endeavour. Thank you all for believing in me and being part of this significant milestone in my academic career.

Table of Contents

List of Tables

List of Figures

List of Symbols

ECD	Equivalent Circular Diameter (ECD)
A_P	projected area
D_H	Hausdorff fractal dimension
D_P	Perimeter fractal dimension
D_V	Volume fractal dimension
D_S	Surface fractal dimension
A	Projected area
P	Particle perimeter

Chapter 1. Introduction

1.1. Coagulation Dosing Control Systems and Current Requirements

Coagulation and flocculation are essential processes used in water and wastewater purifying for removing various pollutants, including organic compounds, suspended inorganic precipitates, colour, and other water contaminants. It is estimated the size of the worldwide coagulant market to be valued at USD 14.76 billion in 2030 (Global Coagulant Market Size and Forecast to 2030, n.d.). Optimizing the chemical dosage in wastewater treatment is a way to reduce operational costs. By carefully adjusting the amount of chemicals used, wastewater treatment plants can achieve cost savings while maintaining regulatory compliance and ensuring effective treatment (Chemicals / Process Optimization - AMCON Europe s.r.o., n.d.). Overdosing chemicals can lead to unnecessarily high material costs and exceed financial budgets while underdosing can decrease treatment efficiency (Chemicals / Process Optimization - AMCON Europe s.r.o., n.d.). The amount of coagulant needed to achieve the desired treatment efficiency relies heavily on various factors. These factors are temperature, pH, effluent quality, coagulant dosage, coagulant type, and the mechanisms associated with different natural coagulants (W. Li et al., 2022; Saritha et al., 2017). Additionally, the hydraulic characteristics of the treatment steps, such as rapid mixing, play a crucial role in determining the best coagulant dosage (Rosińska & Dąbrowska, 2021).

Currently, the prevailing approach for regulating coagulant dosage in wastewater treatment plants relies on a flow-proportional dosing strategy. This approach involves adjusting the coagulant dose based on the flow rate of the water. The disadvantage of the flow-proportional dosing strategy for coagulation control is that it may not always account for variations such as pH, alkalinity, turbidity, and organic loading, which can impact the coagulation efficiency (Ratnaweera & Fettig, 2015a). This can lead to suboptimal dosing and potential over- or under-dosing of coagulants, impacting the treatment process and resulting in increased chemical usage or excess produced sludge (Malcolm J. Brandt, 2016). Therefore, while flow-proportional dosing is a valuable approach, it has limitations in addressing the dynamic nature of water quality and may benefit from complementary control strategies to optimize coagulation dosage.

Advanced multi-parameter-based coagulant dosing control systems utilize online measurements and multivariate analysis to enhance the efficiency of coagulant dosage in water treatment procedures (L. Manamperuma et al., 2017). These systems are designed to address the limitations of flow-proportional dosing by considering multiple parameters such as pH, organic loading, and temperature (W. Liu & Ratnaweera, 2016; Matilainen et al., 2010). By integrating these measurements, the coagulant dosing control systems can provide more adaptive and real-time adjustments to the coagulant dose, leading to improved coagulation efficiency, reduced chemical consumption, and enhanced outlet water quality.

However, it is important to note that while these systems have shown significant improvements in reducing coagulant consumption and enhancing outlet water quality, their implementation may require an initial investment in terms of equipment and training (W. Liu & Ratnaweera, 2016). Additionally, the complexity of these systems and the need for regular maintenance and calibration could be considered potential drawbacks (Matilainen et al., 2010). Furthermore, the effectiveness of these systems may depend on the accuracy and reliability of the online measurements and the quality of the data used for multivariate analysis. Therefore, while advanced multi-parameter-based coagulant dosing control systems offer substantial benefits, their successful implementation and operation may require careful consideration of these potential drawbacks.

1.2. Objectives

Considering all of the above, it is imperative to develop a smart solution that can accurately predict optimal dosage and replace costly and complicated in-situ sensors. It may also be necessary to develop new sensors to provide decision support and warning systems. There is no doubt that the above-mentioned Advanced Multiparameter-Based Systems are very effective, however, in the context of coagulation, image analysis has been studied several times, but has not been applied in an operational setting. Recent progress in image analysis methodologies and statistical techniques has offered a chance to create an alternative to current methods that are both technically robust and conceptually sound.

Therefore, this research aimed to create two models: one utilizing MATLAB and Python software for training an artificial neural network (ANN) model to predict optimal chemical dosage and another employing the Response Surface Method (RSM) to forecast optimal dosing. As mentioned earlier, the objective of this approach is to improve the effectiveness and cost-effectiveness of advanced coagulant dosing control systems based on multiple parameters., while also boosting automation and treatment effectiveness in WWTPs. It was hypothesized that coagulation conditions would impact the morphology of the flocs.

1.3. Research and Thesis Outline

The research comprised four distinct stages. In the initial phase, the optimal coagulant dose was determined, while the subsequent stage involved the introduction of polymers (flocculants) to evaluate their impact on phosphorus removal. Additionally, images were captured and subjected to MATLAB for image processing. The research process unfolded through the following key steps:

1. Determination of optimal coagulant dosage:
    - Dosing iron salts under specific conditions to identify the optimal coagulant dose.
2. Evaluation of produced sludge and Phosphorus Removal:
    - Introduction of polymers (flocculants) to assess their impact on phosphorus removal and the amount of generated sludge.
3. Developing a mathematical and statistical model
    - Employing response surface methodology (RSM) to optimize phosphorus removal and produced sludge.
4. Image processing in order to find the correlation between flocs sizes and chemical consumption:
    - Selection of a suitable method for coagulation image analysis

This structured approach allowed for a comprehensive investigation into the interplay of coagulants, polymers, and phosphorus removal, supported by quantitative analysis through image processing and mathematical modelling.

Chapter 2. Literature Review

2.1. Coagulation

In the context of wastewater treatment, surface charge refers to the electric charge present on the surface of particles in wastewater. This charge affects the behaviour of particles in suspension and their interaction with other substances. In raw wastewater, most colloidal particles have a negative surface charge. The colloidal particles are constantly colliding in the water due to their Brownian motion and Van der Waals forces. If these collisions do not result in aggregates, the suspension will remain stable. The primary reasons preventing aggregation include:

1. Electrostatic Stabilization: Since particles in wastewater often carry a negative charge, electrostatic repulsion occurs when particles with similar charges approach each other.
2. Steric Stabilization: Certain substances, like polymers, have the ability to adhere to particle surfaces, creating a protective coating. This coating acts as a barrier, inhibiting particles from coming too close to each other. Steric stabilization prevents the attractive forces that could lead to aggregation (Bache & Gregory, 2007; Bratby, 2016).
3. When the particles are no longer repelled by each other, allowing them to collide and adhere, this refers to Coagulation. Following coagulation, flocculation occurs. Flocculation involves gentle stirring or mixing to encourage the growth of larger particles through contact with each other.

Coagulation is a water and wastewater treatment process where positively charged coagulants are added to destabilize and neutralize colloidal particles via electrostatic attraction between the coagulant and counter-ions. Coagulants cause fine particles to come together, forming larger aggregates or clusters called flocs. Since flocs are denser than medium, they settle more readily or can be more effectively separated during subsequent treatment steps. The most frequently employed coagulants in wastewater treatment include aluminum-based coagulants such as aluminum sulfate (Alum; $Al_2(SO_4)_3$) and polyaluminum chloride (PAC), as well as iron-based coagulants like ferric chloride (Ferric; $Fe(Cl)_3$) and ferric sulfate ($Fe_2(SO_4)_3$). In addition to these traditional metal coagulants, synthetic coagulants and biopolymer coagulants are used as well. Coagulation is the initial step in the process, where destabilized particles in the water are brought into contact with a flocculating agent. The flocculant helps to bind the particles together, making them more susceptible to flocculation. Once flocs have formed, they are typically removed through processes such as sedimentation, filtration, flotation, and precipitation with sand and polymer, where the flocs settle out of the water or are separated using physical barriers. Colloidal particles in wastewater consist of non-settleable organic matter, clay particles, plankton, bacteria, small particles of decayed plant material, and other dispersed moieties in the colloidal range. Colloidal solids do not dissolve in water, and their small size prevents them from settling out of the water by gravity. Due to their low sedimentation speed, the most effective method for removing them is coagulation. The coagulation-flocculation process is commonly used to remove suspended particles, turbidity, organic matter, colour, pathogens, and viruses in various water treatment applications, including drinking water supplies, and industrial and domestic wastewater treatment. In municipal wastewater treatment, the principal objective of coagulation is the removal of particles and phosphates. Some of the challenges that can be addressed by coagulation-flocculation are natural organic matter removal (Matilainen et al., 2010), oily wastewater treatment (Zhao et al., 2021), treatment of pulp and paper mill wastewater (Teng et al., 2014), wastewater treatment of paper and cardboard recycling industry (Gholami et al., 2022), treatment of textile industry wastewater (Raj et al., 2023), treatment of Acid red 73 dye and real textile wastewater (Jorfi et al., 2016).

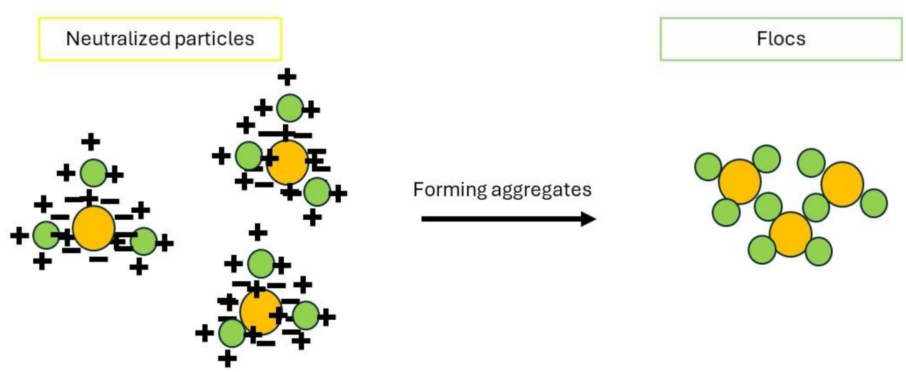

Figure 2.1. Mechanism of particle neutralization and floc forming

2.1.1. Hydrolysis of Metal Salts

The commonly utilized multivalent metal ions in removing suspended solids and phosphates (p) include calcium, aluminum, and iron. The addition of a metal salt to a colloidal system produces several simultaneous and successive chemical and physical reactions. Due to the pH shock and dilution caused by the above process, the metal salt undergoes hydrolysis reactions. The metal ions quickly associate with water molecules, forming hexaaquo aluminum $[Al(H_2O)_6]^{3+}$, which then undergo a series of rapid hydrolytic reactions to generate charged polymeric or oligomeric hydroxo-complexes with diverse structures (Yang et al., 2006). Many researchers have proven that they are essential for particle destabilization (Ratnaweera et al., 1992a). When employing standard coagulants such as $Al_2(SO_4)_3$ or $FeCl_3$, it is observed that amorphous hydrolysis species, specifically Al(OH)3 or Fe(OH)3 emerge in wastewater treatment systems (Jiang & Graham, 1998a). The aqueous chemistry of Al is complex and upon the addition of an Al coagulant in water treatment, multiple reaction pathways are possible. For example, coordination between Al and inorganic ligands (e.g. PO43-, F-, OH-, SO42-) and organic ligands (e.g. humic materials) can occur as parallel competitive reactions. In addition, serial formation of Al monomers, Al polymers and AI(OH)3(s) may take place, depending on pH (Van Benschoten & Edzwald, 1990). Therefore, chemical-equilibrium-based models, which predict fixed equilibrium residual phosphorus concentration, are not suitable for calculating chemical sludge formation and residual phosphorus concentration (Szabó et al., 2008).

2.2. Flocculation

Polymers engage in destabilizing actions by adsorbing onto the surface of polluting particles and forming bridges between the polymer and the particles (Hjorth & Jørgensen, 2012). This adsorption process involves the attachment of polymer molecules to the colloidal particles, leading to the creation of bridges between the polymers and the particles. These polymer-particle bridges contribute to the aggregation of colloidal particles, facilitating the formation of larger aggregates or flocs. It is important to note that the use of flocculants not only enhances the density and solidity of the flocs formed, but also decreases coagulant consumption (Radoiu et al., 2004). Furthermore, it improves the reliability of the treatment process and increases the capacity of treatment plants.

Polymers can serve as coagulant aids, playing a valuable role in enhancing the efficacy of coagulation processes (Lee et al., 2014). This cooperative action results in improved particle removal during the coagulation process. The use of polymers as coagulant aids is a strategy employed to optimize the overall performance of coagulation in water and wastewater treatment, ensuring more efficient and thorough purification of the fluid. The flocculation mechanism of polymers is determined by factors such as charge density, the structure (linear versus branched), amount of charge, charge type and composition, molecular weight, and conformation, with different mechanisms such as bridging and electrostatic patch flocculation coming into play at varying charge densities (Maćczak et al., 2020; Sahu & Chaudhari, 2013). Three types of polymers find application in wastewater treatment concerning charge, each serving specific purposes including cationic polymers, anionic polymers or nonionic (Sahu & Chaudhari, 2013). Cationic polymers are used in wastewater treatment due to their positive charge, which makes them well-suited to remove organic solids from wastewater solutions. They are effective in neutralizing the negatively charged particles in wastewater, causing them to agglomerate and form larger particles.

2.2.1. Hydrolysis of Polymers

Polymeric flocculation represents a highly intricate physiochemical process, making a qualitative explanation challenging. Multiple mechanisms play pivotal roles in this process, and given that flocculation significantly shapes floc structure, it is essential to discuss these mechanisms in detail. flocs formed through the bridge mechanism differ markedly from those formed through charge-patch neutralization (Shouci Lu et al., 2005). These mechanisms will be explored more comprehensively later in this chapter. Notably, flocs formed through the bridge mechanism, once broken by shear, may not readily reform due to the rearrangement of adsorbed polymer chains (Shouci Lu et al., 2005). On the other hand, when charge neutralization emerges as the dominant mechanism, shear-broken flocs can be reformed upon reducing shear (Shouci Lu et al., 2005).

2.2.1.1. Bridging

Bridging phenomena are linked with high-molecular-weight polymers where the tails and loops of the macromolecule can establish connections between particles. Upon optimal dosing of a polymer macromolecule, absorption on particles occurs through multiple segments, with other parts of the molecule extending into the solution (see Fig. 2.2.a). Two conceivable types of bridging mechanisms exist, where bridging can occur between two particles linked by the long chain of a single polymer (see Fig. 2.2.b), or two particles can be linked by the association of polymer molecules separately adsorbed on different particle surfaces (see Fig. 2.2.c). The latter scenario may arise when the surface coverage of the polymer is substantial, the loops and tails are extended, and the association between polymer chains is robust. These bridging mechanisms lead to the formation of aggregates, as shown in Fig. 2.2.d. For effective bridging, the macromolecule typically requires an extended configuration with an end-to-end distance. The solution's pH and the presence of polyvalent counterions influence the uncoiling of the polymer, with an increase in ionic strength causing the polymer to coil up and weaken bridging bonds.

In alternative scenarios, the extended portion of the molecule may adsorb onto other sites of the same particle, rendering the polymer incapable of functioning as a bridge (see Fig.2.2.e). This may lead to surface saturation, where no additional absorbable sites are available, resulting in steric stabilization and the redispersion of particles in the solution. Conversely, in instances where flocs may be broken up by agitation, the extended parts of the polymer molecules may re-adsorb on the same particle surface, preventing effective bridging and causing particle redispersion (see Fig. 2.2.f). Kinetics play a vital role in efficient bridging, making it preferable for polymer molecules to adsorb on two or more particles simultaneously.

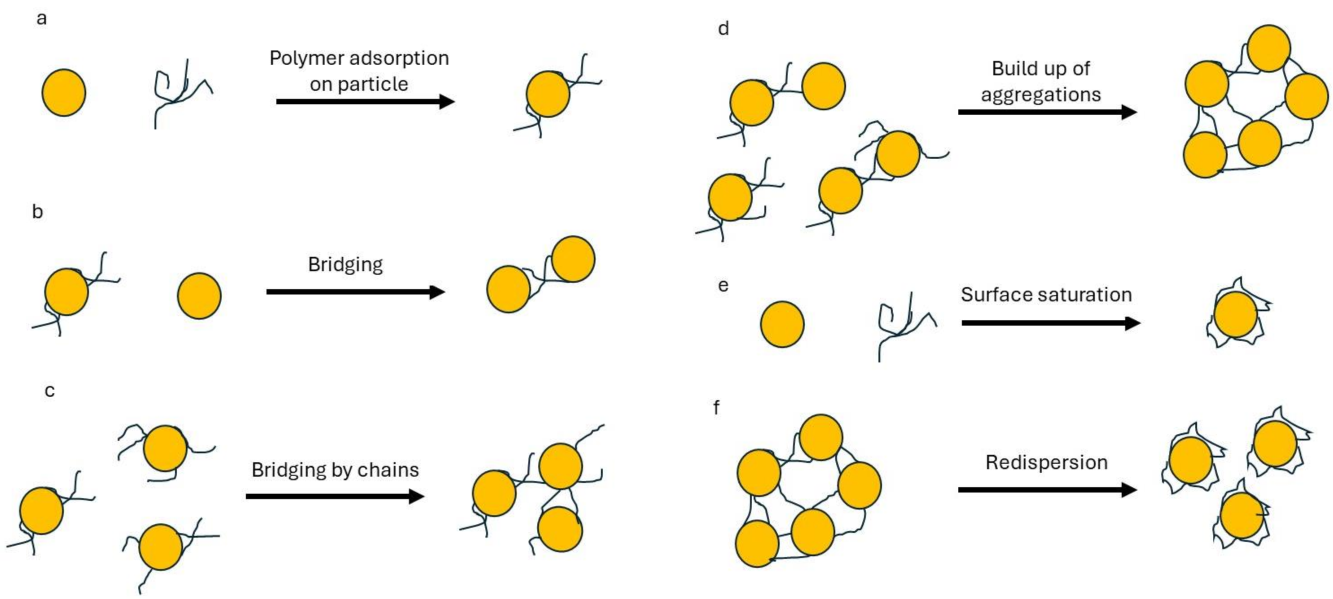

Figure 2.2. illustrating how polymers impact particle adsorption and interactions, ultimately leading to either flocculation or dispersion

2.2.1.2. Charge-Patch Neutralization Process

The initial electrostatic-patch model, as proposed by Gregory, J. (1978), primarily pertains to the flocculation involving cationic polymers with low to moderate molecular weight and high charge density. In this scenario, the charged polymer is envisioned to be considerably smaller than the particle's surface area, creating a patch on the surface. This results in an uneven distribution of surface charges on the particle, leading to the neutralization of surface charges and the induction of an opposite charge based on its charge density. Consequently, patches of charge are dispersed across the particle surfaces. Upon the collision of particles, interactions between oppositely charged patches drive the formation of flocs, as illustrated schematically in Fig.2.3. In such instances, the flocculation mechanism is often likened to the electrostatic coagulation of colloid particles, achieved through the compression of the double layers surrounding the colloid particles (Shouci Lu et al., 2005).

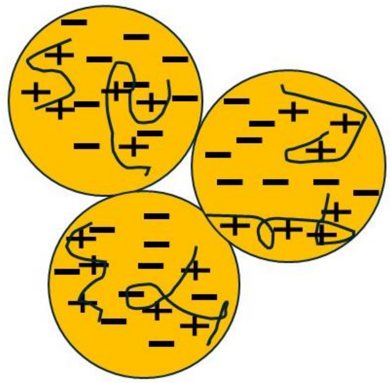

Figure 2.3. Schematic of the electrostatic model leading to aggregation

2.3. Precipitation of Phosphate

Removal of phosphate is important as an excess of phosphates can cause the overgrowth of algae and aquatic plants. Once phosphates enter waterways from various sources such as human and animal waste, industrial effluents, and fertilizer runoff, they can lead to eutrophication, which is the over-fertilization of aquatic plants (D. Liu et al., 2009; Surface Water: Phosphates and Other Waterborne Fertilizers, n.d.). Increasingly strict regulations are being imposed on the removal rates of total phosphorus (total P) in wastewater treatment processes, especially in ecologically vulnerable regions of water bodies. In Manitoba, the limit for total P discharge when releasing wastewater is currently set at 1 mg/L. The coagulation-flocculation process proves highly efficient in the removal of phosphates. This effectiveness arises from chemical reactions with metal ions onto other particles.

The common metal salts are mainly Fe^{3+} salt, Al^{3+} salt and Fe^{2+} salt. These reagents are used in both solution and suspension. The following equations express chemical reactions:

$$Al^{3+} + PO_4^{3-} \rightarrow AlPO_4 \downarrow \qquad (2.1)$$

$$Fe^{3+} + PO_4^{3-} \rightarrow FePO_4 \downarrow \qquad (2.2)$$

Although the general indication of the molar relationship between the metal salt and phosphate in the coagulation process shows that 1 mole of phosphate precipitate by 1 mole of aluminum, Al^{3+} or Fe^{3+}:P ratio is higher in real wastewater treatment. There are several reasons why this ratio is often maintained at higher levels. Different ions or compounds may compete for adsorption onto surfaces, affecting the overall surface charge and interactions between particles. Competing reactions also may lead to the formation of undesired complexes or compounds, altering the chemical equilibrium and potentially reducing the availability of metal ions for phosphorus binding (Luk, 1999).

Although the mechanisms of Phosphate removal during coagulation have been extensively studied in recent decades, the findings are still being questioned. The hydrolysis of metal salts, such as aluminum and iron salts, in water, leads to the formation of various hydrolyzed species, which play a crucial role in the coagulation process. These hydrolyzed species are responsible for the destabilization of particles and the removal of impurities such as turbidity, colour, and phosphate during water and wastewater treatment. Generally, the coagulation of PO_4^{3-} ions with metal ions (Me) occurs through two closely connected mechanisms:

1) the adsorption of PO_4^{3-} ions on Me-hydroxide.

2) the formation of metal-phosphate complexes $Me(OH)_{3-x}(PO4)_x$ (Ratnaweera et al., 1992b).

Studies on the mechanisms of particle and phosphorus removal (L. D. Manamperuma et al., 2016; Ratnaweera, 1991) found that when the concentration of orthophosphates (ortho-P) is constant, higher suspended solids (SS) will result in higher SS removal while decreasing orthophosphates removal efficiency. When the concentration of suspended solids in the influent is high, the hydrolysis of Al(III) ions takes precedence as the primary reaction. In the presence of increased levels of orthophosphates (ortho-P) in wastewater, the prevailing reaction shifts towards phosphate precipitation (L. D. Manamperuma et al., 2016).

Hatton (1985) conducted research using organic polyelectrolytes with inorganic coagulants to enhance treatment efficiency and the characteristics of flocs. They dosed polyaluminium chloride (PAC) and polydiallyldimethylammonium chloride (PDADMAC). In Hatton's study, they found that both PAC and $Al_2(SO_4)^3$ removed orthophosphates equally well when used in the same amounts. However, PAC was more effective because it absorbed more PO_4^{3-} onto the floc blanket. The influence of metal coagulants with organic polymers on the coagulation of domestic wastewater was investigated in a study (Kozminykh et al., 2016). The researchers observed that the dosing of metal coagulants and cationic polymers yielded the most significant removal rates for suspended solids, total chemical oxygen demand, and ortho-phosphates.

Some studies have suggested that a coagulant with a higher OH/Al ratio is associated with an increased dosage requirement for phosphate removal (Boisvert et al., 1997; Diamadopoulos & Vlachos, 1996; Fettig et al., 1990; Jiang & Graham, 1998b; Ødegaard et al., 1990; Ratnaweera et al., 1992c).

2.4. Influential Factors on The Coagulation Process

In the coagulation process, rapid mixing is required as it encourages coagulants to interact with suspended particles and form microflocs. This interaction destabilizes the particles, allowing them to collide and create larger flocs that can be easily precipitated. However, excessive energy consumption during mixing can lead to unnecessary costs and impact the subsequent flocculation process. Amirtharajah & Mills. (1982) determined the type of rapid mixing unit based on the coagulation rate between aluminum hydrolysis products (Al(III)) and colloidal suspensions. As a result of Edzwald's (2013) research, it was found that adequate mixing speed are essential for neutralizing charge and coagulating the coagulated matter in "sweep floc". According to him, reducing energy and cost can be achieved by selecting the right mixing speed and design, based on the coagulation mechanism. The key findings of his study are:

- Intensive mixing and short mixing times are required for the charge neutralization mechanism.
- The significance of the velocity gradient for the sweep-floc mechanism is negligible. it is essential to achieve a uniform coagulant concentration in the mixing volume.

Unlike rapid mixing, which initiates the dispersion of coagulants and the formation of microflocs, slow mixing focuses on fostering the growth and maturation of these microflocs into larger or settleable macroflocs. Well-formed and matured flocs, a result of slow mixing, have an increased capacity to capture and incorporate additional suspended particles, crucial for effective impurity and contaminant removal. Mixing speed, retention time, the mass of the floc, and settling time distribution were taken into account (Ødegaard H, 1985) to optimize floc separation performance. The preferred method is a three or more-step flocculation process which includes:

- Shorter flocculation at higher intensity
- Longer flocculation at lower mixing speed
- shorter flocculation at the slower possible mixing to minimize the possibility of settling.

In another study conducted by Parker et al. (1970), they explored the maximum floc sizes under varying mixing speeds and concluded that floc disruption is influenced by an energy cascade transfer. The pre-polymerization extent of the coagulant affects the coagulation process. With an increase in the OH/Al ratio of the coagulant, equivalent orthophosphate removal rates were obtained by applying a higher dose (Fettig et al., 1990; L. D. Manamperuma et al., 2016; Ødegaard et al., 1990; Ratnaweera, 1991; Zouboulis et al., 2007).

Temperature is one of the key parameters that significantly impact the process's overall performance. Temperature influences the kinetics and thermodynamics of chemical reactions, playing a crucial role in the coagulation-flocculation process. The rate of chemical reactions generally increases with temperature due to enhanced molecular motion and collisions. Fitzpatrick et al. (2004) showed that floc formation is slower at lower temperatures for all coagulants, and higher temperatures can enhance the reaction rate, affecting coagulation and flocculation efficiency. According to Kang & Cleasby. (1995), temperature has the potential to influence several key aspects of the coagulation process, including the hydrolysis of metal salts, adsorptive behaviour, the movement of particles, interactions between particles, flow rates, and precipitation speed. The debate persists regarding whether the reduced efficiency of coagulation at lower temperatures is primarily due to chemical factors or processes related to particle transportation. In a study by Xiao et al. (2009), a significant difference was observed between 2°C and 22°C in the growth rate of flocs. The authors proposed that this difference might be attributed to hindered Brownian motion. Furthermore, they investigated the sedimentation of flocs at different temperatures and noted finer settling at lower temperatures. However, the settling speed was slower under these conditions. To address this issue, they proposed a solution involving the enhancement of particle collision frequency, thereby the increase in turbidity increases floc growth rate.

It is obvious that the influent wastewater characteristics change during each month. In the warm months, people are used to utilizing more water for their daily activities while on colder days their water usage pattern changes. Moreover, In the morning, we can expect an increase in the influent entering the wastewater plants. It experiences a decrease during working hours and undergoes an increase in the evening, then gradually declines during the night. Hence, it is expected to fluctuate in the inlet turbidity behaviour, wastewater solids, pH, conductivity and temperature. In periods of rainy days or snow melt, the characteristics and volumes of incoming water exhibit rapid changes.

2.5. Influential Factors on The Flocculation Process

2.5.1. Polymer Dosage

The effect of polymer dosage on flocculation is a critical factor in water treatment. It is well known that an optimum amount of polymer is required for flocculation and the flocs may break up more easily at a too high rate of addition. This may lead to insufficient mixing in the suspension leading to ineffective flocculation. Much research has shown that dosing polymer to improve floc characteristics is a widely practiced method to enhance floc strength. The use of polymers as coagulant aids in combination with metal ions has been studied to improve coagulation and flocculation performance. Nti et al. (2021)conducted research using polyaluminum chloride (PAC) as a polymer to enhance coagulation in combination with Alum. Their results revealed that lower dosages are more effective, thereby potentially reducing the costs of the process. Zarei Mahmudabadi et al. (2018) have shown that the application of polymers as coagulant aids can decrease the efficient dose of PAC coagulant. They also proved that The removal efficiency of polymers decreased with an increase in concentration above their optimal dose.

2.5.2. Influence of pH and Ionic Strength

The influence of pH and ionic strength on the process of flocculation holds significant importance, impacting the stability and sedimentation of particles (Konduri & Fatehi, 2017). The pH factor plays a crucial role in managing the charges present on both the polymer and particle surfaces. An increased density of similar charges on both surfaces can result in repulsion. Ionic strength is equally vital, as the compression of the double layer leads to a reduction in the separation between particles, instigating flocculation through mechanisms like charge patch and bridging flocculation (Shouci Lu et al., 2005). Fig. 7.12 presents a good illustration of the effect of pH on the organization of adsorbed polymer on clay surfaces across the pH range. At pH 4.4, a pH at which the surface charge of the clay is small, the polymer is adsorbed with the chain train closely associating the many surface sites to give cross-linked bridges with strength. At pH 7, when negative charges on the clay surface increase and promote the dissociation of the polymer, the loose polymer coil undergoes additional electrostatic repulsion and adsorbs as loops. The process of bridging links resulting adsorbed polymer chains and forms large flocs. At pH 9, where the clay charge is increased further and repulsion between particles and the polymer is intensified, the polymer coils adsorb and bridge from adsorbed (adsorbing) particles. With the tails of chain extended, polysilicate ions combine with polymer bridges to form multi-particulate boundaries of thick, porous, very weak flocs (Shouci Lu et al., 2005).

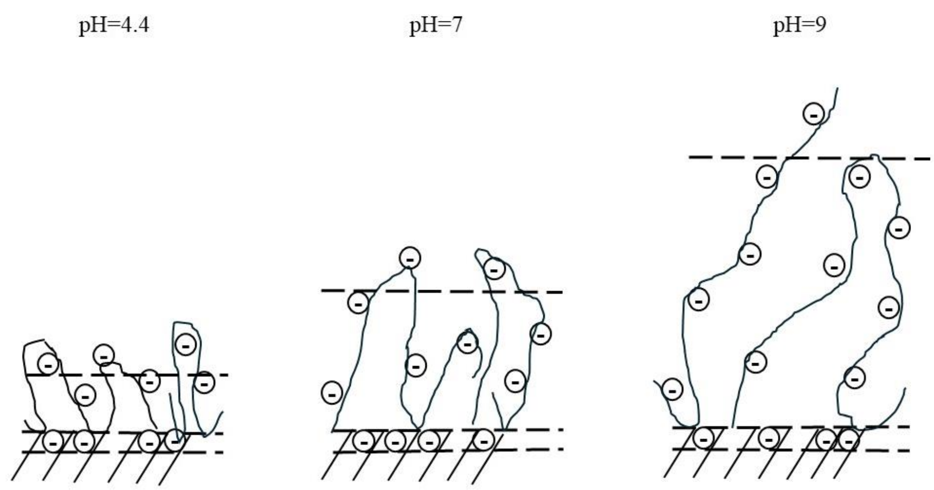

Figure 2.4. Effect of pH on flocculation

Brij M. Moudgil & Bernard J. Scheiner. (1988) and Somasundaran et al. (1996) conducted a comprehensive investigation into alumina flocculation using a pyrene-labeled PAA polymer. The outcomes of their research were notably considerable. At a pH level of 10, the polymer, once adsorbed, demonstrated a stretched conformation that extended into the solution. Conversely, a reduction in pH to 4 resulted in the absence of coiling in the adsorbed polymer. It became clear that there is a potential way to enhance the efficiency of flocculation within the system.

2.5.3. Shear Degradation of Polymers In Solution

Shear degradation of polymers in solution refers to the irreversible breakdown of polymer macromolecules due to mechanical forces, leading to a loss in viscosifying power. This degradation can occur during various stages, such as high agitation during mixing, the use of high-shear pumps (Mackenzie & Jemmett, 1971). Although some shear degradation is inevitable, understanding the effect of shear rate on the polymer system may help to reduce it. Other factors such as shear time, concentration, polymer type and ionic strength can influence the polymer structure (Shouci Lu et al., 2005). Henderson & Wheatley. (1987) carried out an extensive study on the loss of flocculation efficiency of polyacrylamide flocculants. Their investigation disclosed that the shear degradation of polyacrylamide solutions leads to a decline in intrinsic viscosity, consequently diminishing flocculation activity. Furthermore, their findings highlighted that, under a consistent shear rate, minimizing molecular degradation could be achieved through; (i) minimizing the duration of exposure to shear; (ii) maintaining a low solution concentration; (iii) ensuring a high ionic strength of the solution; and (iv) having a high percentage of anionic charge in the polyacrylamide.

2.5.4. Polymer-Cation Complex Formation in Solution

The formation of polymer-cation complexes in solution affects floc size by promoting the aggregation of particles and the subsequent formation of larger flocs. Cationic polymers, through the formation of complexes with negatively charged particles, facilitate the bridging aggregation of particles, leading to the growth of flocs and the production of larger floc sizes (Zhou & Franks, 2006). The dosing of polymer to improve floc characteristics is a widely practiced method in water treatment, and it has been shown that at low dosages, the floc size is expected to be very small due to an insufficient amount of polymer adsorption on the particle (Deniz, 2015). Therefore, the formation of polymer-cation complexes significantly influences floc size, with the complexes playing a crucial role in promoting the growth of flocs and enhancing the overall efficiency of the flocculation process.

2.6. Dosing Control Strategies

The Jar test is a standard laboratory procedure employed to establish the optimal amount of coagulants, pH, and temperature to minimize contaminants in raw wastewater during the treatment process. This test is crucial in determining the set points for the coagulant dosage system controller. However, the Jar test has limitations, particularly in responding effectively to rapid changes in raw wastewater characteristics. This drawback makes it unsuitable for addressing such variations in real-time. To implement automatic control in the water treatment process, a robust model that provides a more accurate depiction of the coagulation process is essential for ensuring optimal controller performance.

Effective control strategies are needed to optimize the operations of WWTPs. With modern WWTPs being designed for full automation, the application of computer algorithms has become instrumental in enhancing control functions within plant operations. Two main dosing control strategies proposed in the literature are direct online dosing control and indirect online dosing control, aiming to achieve optimal results in the coagulation process (Ratnaweera & Fettig, 2015b). Direct online dosing strategies are based on online parameter measurement that can be broadly classified into three categories: feedforward, feedback, and feedforward-feedback (American Water Works Association & American Society of Civil Engineers, 2012; Joo et al., 2000).

2.6.1. Direct Dosing Control Strategies

2.6.1.1. Feedforward Dosing Control

In this strategy, the amount of coagulating chemicals required for the treatment is obtained from sensory data from wastewater variables. This generally involves adjusting the feed rate of metering pumps in response to the measured flow rate of raw wastewater (El-taweel et al., 2023). However, this approach becomes inadequate when dealing with rapid fluctuations in flow rates and significant changes in other water quality parameters. Therefore, the coagulant dosage controller cannot show a proper reaction to these changes and its performance decreases.

2.6.1.2. Feedback Dosing Control

In this approach, many sensors such as a streaming current detector, zeta meter, dispersion analysers (PDA) and pH meter are involved to analyze the controlled parameters in the effluent. When the detected value varies from a predetermined setpoint, the controller produces a signal indicating the degree of deviation. This signal is sent to a dosing system, such as a metering pump, and the pump's output is adjusted to maintain the desired wastewater quality. Due to cost of online sensors, the use of software sensors is being proposed to replace these expensive online sensors (El-taweel et al., 2023).

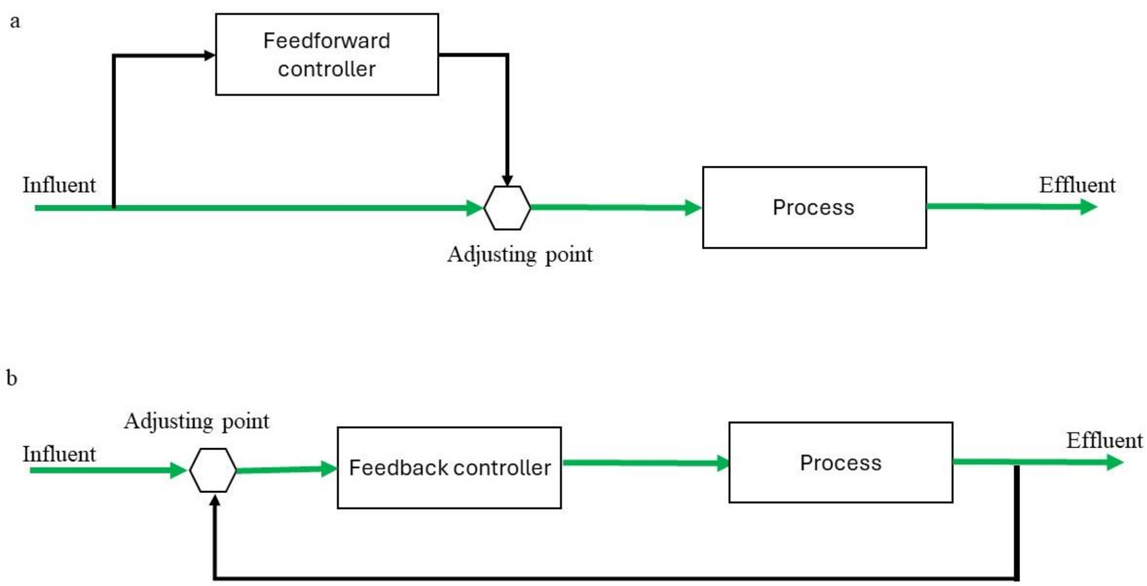

Figure 2.5. Direct dosing control strategies a) Feedforward, b) Feedback

2.6.2. Indirect Dosing Control Strategies

There has been considerable research in recent years evaluating data from jar tests, pilot-plant tests, and full-scale operations using advanced mathematical tools in order to derive relationships between input and output parameters. Although they are not based on a physical understanding of the processes but rather on a mathematical analysis of existing data. There are basically three different approaches to modelling the resulting correlations:

1. Multivariate regression analysis.
2. Artificial neural network models (ANN).
3. Fuzzy logic models.

For dosage control functions, these models can be combined with suitable physical sensors, commonly referred to as virtual sensors or software sensors, in order to achieve the desired results.

2.6.2.1. Multivariate Regression Analysis

MRA is a powerful technique for exploring the relationship between multiple independent and dependent variables. It offers researchers a clear and comprehensive understanding of how changes in independent variables relate to shifts in the dependent variable. AlGhazzawi & Lennox. (2009) as part of their research, they developed a condition monitoring tool for model predictive control that helps users detect abnormal controller operation and resolve abnormalities as necessary. However, they also emphasize that process knowledge and experience are necessary to correctly analyze model predictive control and process abnormalities. (Franceschi et al., 2002a) conducted a comprehensive examination of jar test data using synthetic raw water, which included particles and natural organic matter (NOM), treated with alum. The study encompassed eight key water quality parameters: particle type, initial turbidity, initial UV absorbance, temperature, pH, conductivity, calcium concentration, and sulfate concentration. Employing a two-level fractional factorial design method, the researchers aimed to assess the significance of each parameter concerning both the minimum dosage required and residual turbidity after settling. Their findings revealed an antagonistic relationship among the various input parameters regarding the two studied responses (dosage minimization and residual turbidity), making it impractical to optimize the process simultaneously for both outcomes. Ratnaweera et al. (2002, 2005) proposed an innovative dosage control concept for mechanical-chemical wastewater treatment plants in Norway. They aimed to determine the relationship between coagulant dosage and input parameters such as flow rate, temperature, pH, conductivity, turbidity, ortho-P, settling time, and effluent turbidity, they used technical-scale data and applied partial least square regression analysis. As a result of the first study, DOSCON® (DOSCON AS, Oslo, Norway) was developed as an online control tool. There are still weaknesses in this system due to the reliance on several online sensors, which can be expensive and complicated to operate, and the insufficiencies in feedback control. Trinh & Kang. (2011) conducted jar tests using water sourced from the Nakdong River in Korea, employing response surface methodology to obtain optimal conditions. They utilized a quadratic model to estimate the correlation between coagulant dosage and pH as input variables and turbidity and dissolved organic carbon (DOC) removal as corresponding responses. The coefficients of the model were derived through multiple linear regression analysis. Their findings revealed a narrow pH-dosage range where the removal of both turbidity and DOC was optimal, while the optimal ranges for either parameter alone were considerably broader.

2.6.2.2 Artificial Neural Network Models (ANN)

As a nonlinear regression method, neural networks can be used as a tool for predicting historical data by identifying patterns. Various types of neural networks are distinguished by their architecture; backpropagation feedforward neural network (FFNN) which is known as multilayer perceptron (MLP) is one the most popular used approach. ANN models are constructed by dividing them into three stages: training, validation, and testing. As a result, the data set is divided into three classes. The training data set generally comprises 70–80% of the data, while the remaining data is split between the validation and testing sets. An ANN is constructed by training each of its inputs and outputs. This step is the beginning of the process of constructing the ANN. Each neuron's weight is adjusted at each epoch during the training stage until the stopping criteria is met. There are several possible stopping criteria, such as minimum error values, epoch count, or iteration and validation checks. Following the training stage, a validation dataset is used to test the predictive ability of the ANN model. The validation process involves several validation checks to ensure that the model does not fall into a local minimum.

Zheng et al. (2011) conducted a study by using domestic wastewater in jar tests. A neural network model based on the results was developed for COD removal, using initial pH, coagulant dosage, P/Al ratio, and agitation speed as input parameters. In addition, a photographic image analysis technique was used to analyze the flocs. This study found that the ANN was only able to predict the coagulation efficiency to some extent because there were insufficient experimental data points. Due to the absence of direct accounting for raw water load, it is uncertain whether the selection of input parameters was optimal here. An MLP neural network model was created by(Zhang & Luo, 2004) using data from the full-scale operation of a waterworks in China, using raw water temperature, pH, and turbidity as input parameters, coagulant dosage as output, and streaming current signals as output parameters. By using their system, the treatment plant could save significant amounts of coagulant. The search did not return specific disadvantages of using ANNs in coagulation.

2.6.2.3 Fuzzy Logic Models

Fuzzy logic models in wastewater treatment involve the application of fuzzy logic, a mathematical approach that handles uncertainty and imprecision, to optimize and control various processes within wastewater treatment systems. These models are employed to optimize the performance of different treatment processes. These models can consider multiple input variables and their interdependencies, allowing for more nuanced control strategies. For instance, fuzzy logic can be applied to optimize the dosages of coagulants and flocculants based on changing influent water characteristics. Chen & Hou. (2006), Taiwanese researchers, developed a feed-forward control system with a fuzzy feed-backward system for a drinking water treatment plant. To develop the fuzzy control rules, full-scale data were collected over a period of four years, and pH as well as turbidity in settled water were used. Many field tests were conducted to demonstrate the effectiveness of the proposed strategy.

2.7. Response Surface Methodology

It is not always possible to use a theoretical model to describe how some independent variables (factors) relate to a dependent variable (response). In these cases, information about the relationship between factors and response should be obtained empirically. Response Surface Methodology (RSM), introduced by(Box & Wilson, 1992), consists of a collection of mathematical and statistical techniques for modelling and analyzing problems in which the response of interest is influenced by a variety of variables (Douglas C. Montgomery, 2008). This methodology follows two main objectives:

- To obtain a prediction of the observed response within the experimental domain in which experiments were not conducted, as precisely and precisely as possible.
- To optimize responses

For example, an environmental engineer wishes to optimize the amount of coagulant (x_1) and flocculant (x_2) that maximizes phosphorus level (y) while it is under 1mg/l. Hence the response can be expressed as:

$$y = f(x_1, x_2) + \varepsilon \tag{2.3}$$

The dependent variable y is a function of x_1, x_2, and the experimental error term, denoted as ε. The error term ε represents any measurement error on the response, as well as other types of variations not counted in f. Typically, the modeller starts with a low-order polynomial in a small region to develop an approximation for the true response function f in RMS problems. The approximating function is a first-order model if a linear function of independent variables can be used to define the response. A first-order model with 2 independent variables can be expressed as:

$$y = \beta_0 + \beta_1 x_1 + \beta_2 x_2 2 + \varepsilon \tag{2.4}$$

When the response surface has a curvature, a higher degree polynomial is needed. A second-order model approximates the response surface by using two variables:

$$y = \beta_0 + \beta_1 x_1 + \beta_2 x_2 + \beta_{11} x_{11}^2 + \beta_2 x_{22}^2 + \beta_{12} x_1 x_2 + \mathcal{E} \tag{2.5}$$

2.7.1. Second-Order Model

When a first-order model is not sufficient, it indicates that the system's behaviour is more complex than what can be adequately captured by a single-order mathematical representation. In such cases, where higher accuracy or a better fit is required, an alternative second-order modelling approach can be considered. Second-order models introduce additional parameters that provide increased flexibility in describing the system's response. It is expressed as below (Box & Wilson, 1992):

$$y = \beta_0 + \sum_{i=1}^{q} \beta_i x_i + \sum_{i=1}^{q} \beta_{ii} x_i^2 + \sum\sum_{i<j} \beta_{ij} x_i x_j + \mathcal{E} \tag{2.6}$$

This model describes quadratic surfaces with various characteristics such as minimum, maximum, ridge, and saddle points. These surfaces represent the behaviour of a function in different directions. Stationary points, where the gradient is zero, are crucial in optimization, indicating potential optimal solutions. Engineers and researchers use these concepts to fine-tune parameters for the best outcomes in applications like engineering design and machine learning algorithms (Box & Wilson, 1992). So the three-factor levels, such as Box-Behnken Design (BBD), Doehlert, three-level factorial, and central composite design are used to evaluate the response.

2.7.1.1. The Central Composite Design (CCD)

CCD is the most frequently used and the most popular second-order design for coagulation of wastewater treatment. As previously mentioned, this was first introduced by (Box & Wilson, 1992). Many studies have used CCD to optimize desired variables. Benalia et al. (2024) carried out laboratory-scale experimental tests to predict the amount of removed turbidity and Total suspended solids and applied its result to the pilot project. They showed their model was able to predict as accurately as 97.93 % and 98.95 % removal percentage efficiency for turbidity and TSS, respectively. Asadi-Ghalhari et al. (2023) applied a five-level design through the application of a central composite design to investigate the impact of key influential factors on the elimination of turbidity in water solutions using a poly aluminum chloride coagulant and rice starch as a natural coagulant aid. Four primary factors, namely rice starch dosage (mg/L), poly aluminum chloride dose (mg/L), pH, and turbidity, were considered in the investigation. Mensah-Akutteh et al. (2022) used a second-factorial central composite design (CCD) to optimize turbidity and colour removal in the experimental tests. They defined the coagulation conditions variables as alum dose (mg/L), pH and alkalinity (mg/L).

Although the Central Composite Design (CCD) is recognized as a robust approach for optimizing experimental tests, it is not without limitations. One limitation is its potential demand for a substantial number of experiments, especially when dealing with a high number of input factors or when the star points are situated far from the center. Another drawback emerges when incorporating two or more categorical factors, as the method struggles to effectively design tests under such circumstances. The primary and notable limitation pertains to the requirement that the distances among the levels within a factor must be uniform; any deviation from this condition can compromise the effectiveness of the method.

2.7.1.2. Box- Behnken Design (BBD)

The other type of experimental design used in response surface methodology (RSM) is Box-Behnken. Its main purpose is to accommodate the fitting of second-order models which is the primary interest in most RSM studies. This design stands out by assigning each factor three equally spaced values, commonly denoted as -1, 0, and +1. this method can create a quadratic model that includes squared terms, combinations of two factors, linear terms, and an intercept.

Yateh et al. (2023) employed Box–Behnken design to optimize three independent parameters including pH, temperature, and coagulant dosage. They investigated the efficiency of coagulation water treatment processes to remove total organic carbon (TOC), total nitrogen (TN), and total suspended solids (TSS) from urban drinking water. Daud et al. (2018) conducted a study to optimize the coagulation-flocculation process for treating biodiesel wastewater using the Box-Behnken design. Alum dosage (g/l), Initial pH, Rapid mixing rate (rpm), and Settling time (min) were chosen as modelling factors and the experimental and predicted values for turbidity, COD, and SS removal were compared. The results showed that the quadratic model was found to be the most suitable fit.

The Box-Behnken design, despite its utility in response surface methodology, is not without limitations and drawbacks. One notable consideration is the need for center points to enhance accuracy, particularly when predicting responses at extreme factor combinations. Additionally, the Box-Behnken design is not well-suited for experiments involving categorical factors. It is primarily designed for continuous factors, and incorporating categorical variables may lead to suboptimal designs.

2.7.1.3. Optimal Design Method

Optimal design is an alternative to classic RSM design that maximizes the information matrix determinant and is not orthogonal to classic RSM models. This model can be used for any research objective, such as screening or generating response surfaces since it can be used to fit any type of model (first or second order, quadratic, cubic). Furthermore, optimal designs have fewer experimental trials to conduct than classic designs and provide a constrained design space. In these designs, the effects of variables are correlated. This design has the advantage of being extremely flexible and efficient, as it can handle a wide variety of factors, any level of factor settings, and any model specification. The optimal design is also used to reduce generalized variability in parameter predictions for a particular model. Franceschi et al. (2002) studied eight parameters related to natural water quality, using a two-level fractional optimal design to determine their importance. They then varied stirring speed, stirring time and settling time to find the lowest coagulant dose and residual turbidity for each synthetic water.

2.8. Image Analysis of Flocs

Image analysis involves the extraction of meaningful information from images. In the context of floc analysis, image analysis is used to study the characteristics of suspended particles and flocs in water and wastewater. Image analysis of flocs is also a valuable technique for characterizing floc size distributions and understanding the behaviour of suspended particles. Several studies have employed image analysis to study flocs and their properties. The utilization of photographic image acquisition methods enables the real-time capture and analysis of floc images (Chakraborti et al., 2003). The literature has presented various interpretations of floc size. For instance, it could be defined by its length or maximum size, denoting the greatest distance between two points along the floc's perimeter within a single plane. Conversely, some researchers opt for breadth as the size metric, representing the shortest distance between two points on the floc's circumference. Another widely used definition is Equivalent Circular Diameter (ECD), which is obtained by converting the area of an object into a circular diameter value (Bourcier et al., 2016).

$$ECD = \sqrt{\frac{4A_p}{\pi}} \tag{2.7}$$

Where A_p is the projected area of the particle. The figure below indicates the ECD for a needle and a plate.

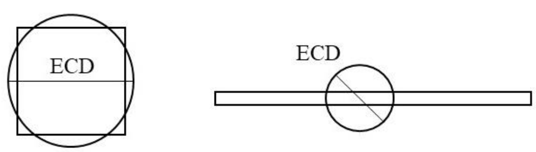

Figure 2.6. ECD for different particles

Many researchers have applied various methods to calculate the size of flocs formed in water and wastewater. Jin. (2005) utilized a high-resolution digital camera to investigate how temperature affects floc properties under varying coagulant dosages in the coagulation of river water. The study revealed the correlations between the projected area of particles and the amounts of coagulant applied. Wang et al. (2011) explored alterations in the characteristics of flocs resulting from varying dosages and coagulation pH in a humic acid suspension, capturing images through a digital CCD camera. The use of image analysis for particle assessment is a well-established technique with a history dating back to (Tambo & Watanabe, 1979). This method has been widely applied in diverse water treatment applications, such as activated sludge processing (Alves et al., 2000; Amaral & Ferreira, 2005; Da Motta et al., 2001; Dagot et al., 2001), aggregates settling velocity measurements (Vahedi & Gorczyca, 2012, 2014), and natural organic matter removal (Xiao et al., 2011). Image analysis applied to coagulation and aggregation of particles was also widely studied in different methods such as Microscopy Image Processing (Ganczarczyk & Rizzi, 1996; D. H. Li & Ganczarczyk, 1989a), Light Scattering (Hilligardt & Hoffmann, 1997; Neis & Tiehm, 1997), Dynamic Image Analysis (DIA) Microscopy (Gorczyca & Klassen, 2008), Optical Imaging by CCD camera (Coufort et al., 2008; Manning et al., 2010).

2.9. Application of Fractal Dimension in Flocs Size Analysis

The term fractal dimension and the associated theory were brought to the fore by the mathematician (B. Mandelbrot, 1967; B. B. Mandelbrot & Wheeler, 1983). D. H. Li & Ganczarczyk. (1989) used fractal dimensions to characterize the spatial structure of the aggregates generated in flocculation/coagulation, activated sludge and trickling filter biofilm processes. It is the most common method for characterizing flocs formed during wastewater and water treatment.

2.9.1. Box-Counting Dimensions Method

Box-counting or box dimension stands out as one of the most commonly employed dimensions. Its widespread use can be attributed primarily to its relatively straightforward mathematical computation and practical estimation. In 1919, Felix Hausdorff introduced an iterative process of subdividing at multiple scales to establish a measure for irregular objects. As this multiscale measure forms the basis for a set of morphological fractal dimensions, these dimensions are named after him (Kinsner, 2005).

$$D_H = \lim_{k \to \infty} \frac{\log(N_k)}{\log(1/r_k)} \quad (2.8)$$

Where N_k the number of elements and r_k size of elements. Equation (2.8) can be used for the calculation of perimeter (D_P), volume (D_V), and surface (D_S). The box-counting fractal dimension utilizes squares and cubes as filling or covering elements in 2D and 3D variations of the Hausdorff dimension. D. H. Li & Ganczarczyk. (1989) conducted research to measure particle sizes of activated sludge in the size range of 30-1000 µm. Their findings indicated that the perimeter fractal dimension of activated sludge flocs fell within the range of 1.13 to 1.22. a few years later another study by Gorczyca & Ganczarczyk. (1996, 1999) prove similar results for alum flocs coagulation. Ganczarczyk & Rizzi. (1996) used same imaging method to obtain surface fractal dimension of activated sludge flocs. They showed surface fractal dimension of activated sludge flocs ranging from was 1.88-1.97 in their research.

If line elements with the size r cover the whole perimeter or boundary of a floc (P) , Eq. (2.8) will result is :

$$P \propto ({}^{1}/_{r})^{D_B} \tag{2.9}$$

Similarly, an equation can be written for the projected area or surface of the flocs.

$$A \propto ({}^{1}/_{r})^{D_A} \tag{2.10}$$

Where A and D_A are the projected area and fractal dimension respectively.

By combining Eq. (2.9) and (2.10), For a 2D floc image, D_P quantifies the correlation between particle surface area and perimeter. (He et al., 2012):

$$A \propto (P)^{\frac{2}{D_P}} \tag{2.11}$$

Where A represents the projected area, while P represents the particle perimeter. For 2D projections of images, A circular-shaped floc has a lower fractal dimension close to 1. On the other hand, a linear-shaped chain of particles has a higher fractal dimension close to 2, indicating a more complex and irregular structure with increased surface roughness.

In previous studies, the morphological details of flocs as a parameter which can control chemical dosing have often been neglected, many studies pay attention directed towards factors such as dosage and influent water quality in modeling (Bi et al., 2024; Lin et al., 2023; P. Liu et al., 2019). However, recent progress in floc morphology analysis, employing methodologies such as fractal theory and image processing, has shown the crucial role of floc structure in determining coagulation-flocculation efficiency which is related to treated water quality (Ren et al., 2017; Yao et al., 2014; Zhong et al., 2011). Additionally, numerous modeling investigations rely on influent parameters from the preceding moment to forecast current effluent quality (Niu et al., 2020; Yaqub et al., 2020), often neglecting the ongoing continuity of the coagulation-flocculation process. Such an approach may not align with the dynamics of real continuous production processes. Molina et al. (2020) introduced a floc characterization method employing image analysis to anticipate settling velocity derived from floc data. This approach contributed to enhancing effluent quality and preventing floc leakage in the effluent. Nan et al. (2009) investigated the fractal dimensions of flocs within the water treatment flocculation process. They integrated macroscopic flocculation effects with microscopic floc shapes. This parameter exhibited a strong correlation with the residual turbidity of raw water across various turbidity levels. Dai et al. (2019) explored the effect of parameters of flocculation performance such as the number of flocs, flocs diameter, and fractal dimensions of flocs on the turbidity removal

Chapter 3. Experimental Methods and Procedures

3.1. Objectives

This chapter aims to conduct bench-scale experimental tests in order to evaluate the removal efficiency of phosphates and to acquire images during coagulation-flocculation in order to analyze flocs morphology at specific periods. Experiments are carried out under different conditions such as various pH's, different temperatures, and different types and dosages of coagulants and flocculants.

3.2. Methodology

3.2.1. Jar Tests

The jar test is a laboratory procedure commonly used in water treatment to simulate the coagulation-flocculation process on a small scale. It involves adding a sample of water to be treated into several jars, along with varying doses of coagulants or flocculants. Bench-scale jar tests were carried out using square beakers with the size of 2 litres on an apparatus. The jar test apparatus consists of paddle stirrers with two rectangular blades on each stirrer, and an electric motor to rotate paddles. Figure 4.1 shows a photo of the bench-scale test equipment.

These jars were mixed at a rapid rate to promote coagulation and flocculation. After a specified mixing period, the agitation was reduced to help form mature and large flocs, and then aggregates were allowed to precipitate. The samples were taken from supernatant water in order to assess the effectiveness of different coagulant doses in removing suspended particles.

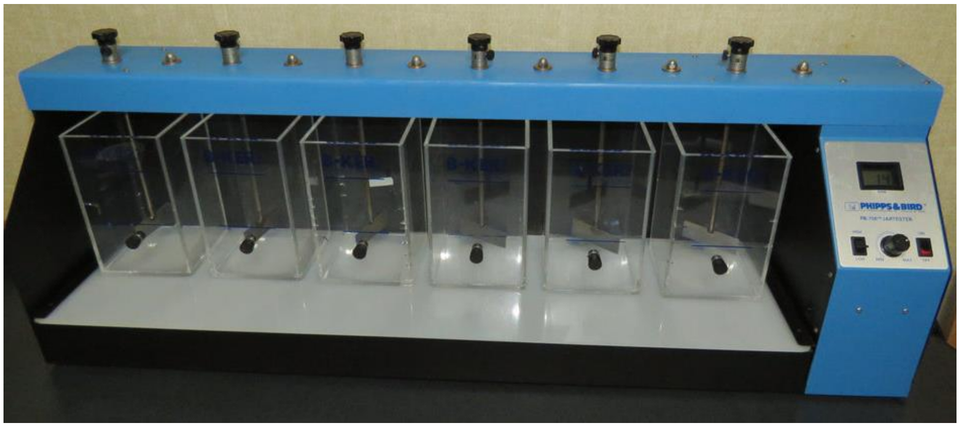

Figure 3.1. Jar test apparatus

3.2.2. Image Acquisition

In the image processing section, one of the mixers was equipped with a black plastic plate with the dimension of 8.5cm*7.5cm which served as a dark background for the flocs. An illustration of the image acquisition is presented in Figure 3.2.

The polymers were added for 4 minutes following rapid mixing. Subsequently, after 1 minute, the agitation speed was reduced, and 15 minutes later, it was stopped entirely. Images were captured starting from the moment the flocculant was applied. The initial image was named picture at 0 seconds, and this process continued until 360 seconds.

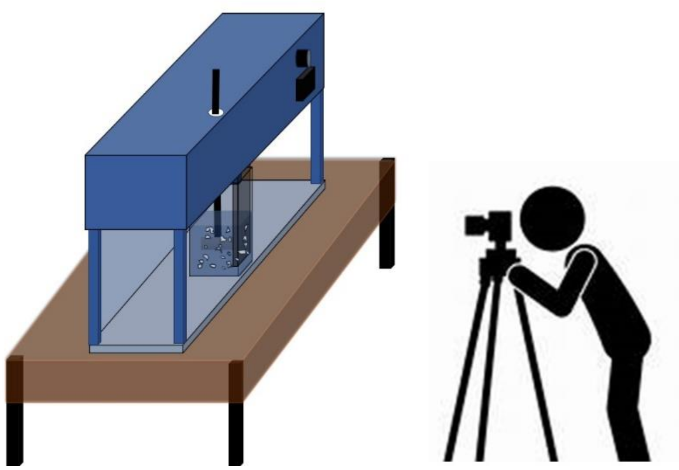

Figure 3.2. An illustration of the image acquisition technique

The image acquisition and storage procedures were managed using the camera control software. All images were saved on the computer's hard drive. Images also were captured using a digital single Canon camera (EOS Kiss X7i Canon) with an EFS 18-135mm Canon Lenz.

The dimensions of the captured image were 1650*950 pixels. A standard frame measuring 8.2cm*5cm was photographed for precise calibration of image sizes. This allowed the determination of the number of pixels corresponding to each standard length for every set of experiments.

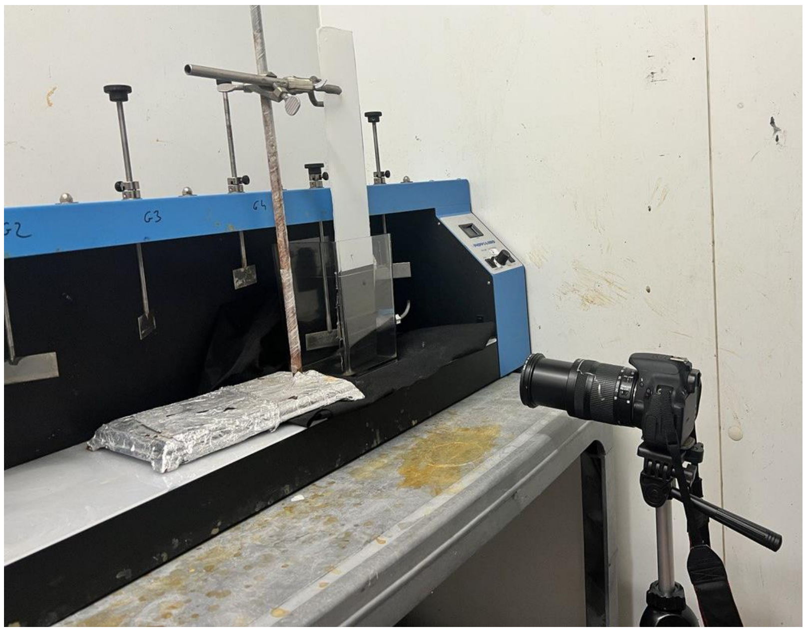

Figure 3.3. Experimental setup for image acquisition

3.3. Experimental Instruments

Table 3.1 shows the instruments used in this study.

Table 3.1. Experimental apparatus

Item	Type
Jar Test Apparatus	Phipps and Bird, PB700
Square Beaker	Phipps and Bird, 2L
Oven	Fisher scientific isotemp oven
Vacuum pump	Gast ,1/8 HP,115 V
Environmental Control Chamber	Conviron

Cold Chamber	Conviron
Digital Camera	EOS Kiss X7i Canon
Lenz	EFS 18-135mm Canon
Computer	Dell, Inspiron 14
Camera Control Software	EOS Utility 3.16.0 for Windows

All of the experiments were conducted inside the chamber in the room E1-231 of the environmental wastewater laboratory at the University of Manitoba under controlled temperatures. In order to protect laptop from cold temperatures it was kept outside of the chamber during the experiments. Figures 3.5 and 3.6 show the chamber and experimental test instruments.

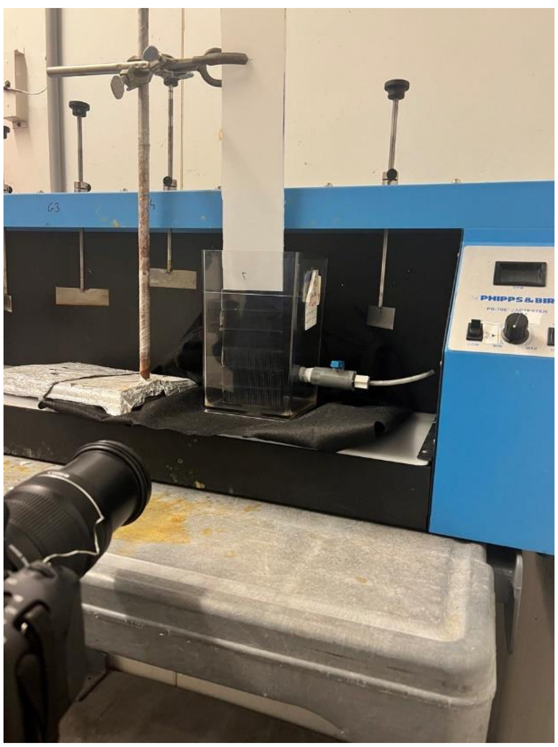

Figure 3.4. Experimental test apparatus

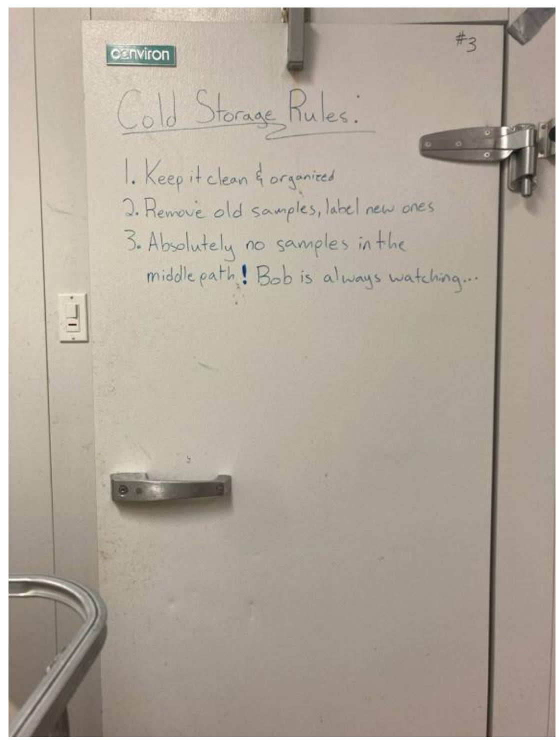

Figure 3.5. Environmental control chamber

Wastewater samples were collected from the secondary cell in RM of Altona wastewater treatment facility and stored inside the cold chamber at 4 Degrees Celsius in the 20-litre pales. Before starting the tests, one pale was taken out of the cold chamber and the wastewater was mixed very well to maintain a consistent sample in terms of suspended solids.

Characteristics of the lagoon wastewater are shown in Table 3.2. All of these parameters are very close to the numbers measured in the University of Manitoba technical lab.

Table 3.2. Wastewater quality and its characteristics

Characteristic	**Wastewater**
pH	7.9
Biochemical Oxygen Demand	10.7 mg/L
Total Phosphorus	3.9 mg/L
Total Organic Carbon	23.8 mg/L
Total Suspended Solids	11 mg/L
Total Nitrogen	63.0 mg/L
Total Kjeldahl Nitrogen	60.4 mg/L
Turbidity	11.8 NTU

Aluminum sulfate and Ferric chloride, which served as coagulants, in water treatment processes, were purchased from CLEARTECH, a renowned supplier known for its quality chemicals. Additionally, cationic polymers including EM440CT, EM840CT, EM440MEB, and EM840MEB, supplied by SNF, further enhance the efficiency of the coagulation process. A stock solution with mixing chemicals and distilled water for both coagulants and flocculants was prepared with the ratio 1:100 and 1:400 respectively. Table 3.3 shows the characteristics of Polymers, Alum and Ferric.

Table 3.3. Characteristics of polymers

Chemical	Bulk viscosity	Viscosity	Specific gravity	Charge density	Molecular weight	Ionic character
EM440CT	500-2000 (cP)	1000 at 5g/L	1.1	High	High	Cationic
EM440MEB	500-2000 (cP)	1800 at 5g/L	1.1	High	low	Cationic
EM840CT	500-2000 (cP)	800 at 5g/L	1.1	Very high	High	Cationic
EM840MEB	500-2000 (cP)	1500 at 5g/L	1.1	Very high	low	Cationic

By manipulating the chamber's temperature settings to specific values, it became possible to precisely control the temperature of the wastewater sample within the chamber. This temperature regulation allowed for adjustments to be made to achieve desired temperatures of 4, 12, and 22 degrees Celsius respectively.

After adjusting the chamber’s temperature, the wastewater sample was placed and remained in the chamber for a duration of 12 hours within the controlled temperature. This temperature adjustment procedure ensured that the sample was exposed to the exact thermal conditions required for the experiment.

Various setups and configurations were experimented with to capture images of flocs during the flocculation process. These setups included testing different parameters such as the use of flash, varying shooting speeds, adjusting focus and zoom settings, and manipulating the distance from the beaker where flocculation occurred. Each configuration was examined to assess its impact on the quality and clarity of the captured images. To mitigate light reflections that could potentially affect image quality, a black cloth was strategically placed around the beaker during the imaging process (Fig 3.6). Additionally, multiple trials were conducted to evaluate the effectiveness of each setup in accurately depicting the morphology and dynamics of flocs as they formed and evolved over time. This systematic approach ensured that the imaging setup employed for floc analysis was precise to enhance the understanding of flocculation phenomena and facilitate a more insightful analysis of floc behaviour.

3.4. Analytical Equipment

Table 3.4 illustrates the analytical instruments and software used in analyzing the experiments.

Table 3.4. Analytical apparatus

Item	Type
pH Meter	Fisherbrand accumet AB315
Balance	Denver Instrument P-403
Phosphate Analyzer	Lachat, Quikchem 8500
Temperature	Maverick Redi-Check Digital Folding Thermometer
Image Analysis Software	Matlab R2023b
Mathematical Modelling Software	Design Expert 13

3.4.1. Flow Injection Analysis

In this study, Flow Injection Analysis (FIA) served as the chosen method for quantifying phosphate levels within treated wastewater. This analytical technique is widely applicable to measure total phosphate concentrations across various water sources, including drinking water, surface water, saline water, and both domestic and industrial wastewater samples. The method's automation streamlines the measurement process significantly, minimizing human intervention and enhancing the efficiency and accuracy of the analysis. To initiate the analysis, we first prepare the reagents, ensuring accuracy and precision in the subsequent measurements. Once the preparations are complete, the samples are loaded onto a standard rack. The analysis begins with the auto sampler, it moves to the designated standard position, extracting the sample for analysis. From there, the sample flows through a series of interconnected components within the system. Initially, it flows through a tube into the pump, facilitating controlled movement and circulation. Subsequently, the sample is directed to a mixing coil, where it encounters colour reagents, dilutants, and acids, leading to the desired chemical reactions. Following this, the sample undergoes further treatment within a heater, promoting colour development crucial for subsequent analysis. Upon exiting the heater, the sample undergoes additional mixing to ensure uniformity. Ultimately, the sample enters the spectrophotometer, a critical component which detects changes in absorption characteristics. The spectrophotometer translates these changes into measurable data, representing phosphate levels within the sample. Lastly, the measured phosphate concentrations are shown as peaks, facilitating easy interpretation and analysis.

Figure 3.6. a) Flow injection analysis instrument and, b) Auto sampler

3.4.2. Measurement of Fractal Dimensions

In image processing, images are often represented as two-dimensional matrices, where each element of the matrix corresponds to the intensity value of a pixel at that particular location in the image. The dimensions of the matrix match the dimensions of the image, with rows and columns representing the height and width of the image, respectively. In a grayscale image, each pixel's intensity is typically represented by a single numerical value, ranging from 0 to 255. A value of 0 indicates the darkest possible shade, which corresponds to black, while a value of 255 represents the brightest shade, which corresponds to white. Intermediate values between 0 and 255 represent varying shades of gray, with higher values indicating lighter shades and lower values indicating darker shades.

$$\begin{bmatrix} 0 & 0 & 0 & 1 & 0 & 0 & 0 & 0 \\ 0 & 0 & 0 & 242 & 0 & 17 & 76 & 0 \\ 0 & 0 & 86 & 125 & 0 & 111 & 57 & 0 \\ 0 & 7 & 236 & 0 & 0 & 179 & 2 & 0 \\ 0 & 113 & 252 & 239 & 169 & 245 & 1 & 0 \\ 0 & 0 & 0 & 20 & 20 & 226 & 0 & 0 \\ 0 & 0 & 0 & 0 & 32 & 147 & 0 & 0 \\ 0 & 0 & 0 & 0 & 26 & 52 & 0 & 0 \\ 0 & 0 & 0 & 0 & 0 & 0 & 0 & 0 \end{bmatrix}$$

Figure 3.7. An example of a matrix and image

In order to perform image analysis of flocs multiple techniques and methodologies are employed to extract meaningful information from images using MATLAB (developed by MathWorks Inc., USA). In the following, the step-by-step process for extracting pertinent features undertaken in analyzing an image is explained.

The initial phase of image analysis starts with defining the path to the input image, which is achieved by amalgamating the folder path with the filename. Subsequently, the image is loaded into memory using the "imread" function, and its contents are stored in a designated variable.

Upon loading the image, the next step is isolating a specific region of interest (ROI) within the image. This is accomplished through a process of cropping, where the image is selectively trimmed to focus solely on the desired area. The defined coordinates of the ROI are [432 110 1063 780]. Following the isolation of the ROI, the image undergoes a transformation to grayscale using the "rgb2gray" function. This conversion simplifies subsequent processing by reducing the image to a single channel representing intensity values, devoid of color information. The grayscale image serves as the foundation for segmentation, a pivotal step in image analysis. Adaptive thresholding is applied using the "imbinarize" function to delineate objects within the image. This technique dynamically adjusts the threshold value based on local pixel intensity variations, thus enhancing the accuracy of object delineation. To refine the segmentation and eliminate extraneous details, morphological erosion is employed. This operation, facilitated by the "imerode" function, shrinks the boundaries of foreground objects, effectively removing small artifacts and noise. Further refinement of the segmented image is achieved through the removal of small connected components using the "bwareaopen" function. This step ensures that only significant objects of interest are retained for subsequent analysis, enhancing the accuracy and reliability of results. To augment the precision of segmentation, active contour segmentation is employed. Active contour segmentation is a technique for delineating object boundaries by iteratively adjusting a contour to minimize an energy functional. The parameter 100 specifies the number of iterations for the active contour algorithm. Finally, the segmented objects undergo feature extraction to quantify pertinent attributes. The "regionprops" function facilitates the calculation of properties such as perimeter and area, providing valuable insights into the characteristics of the identified objects.

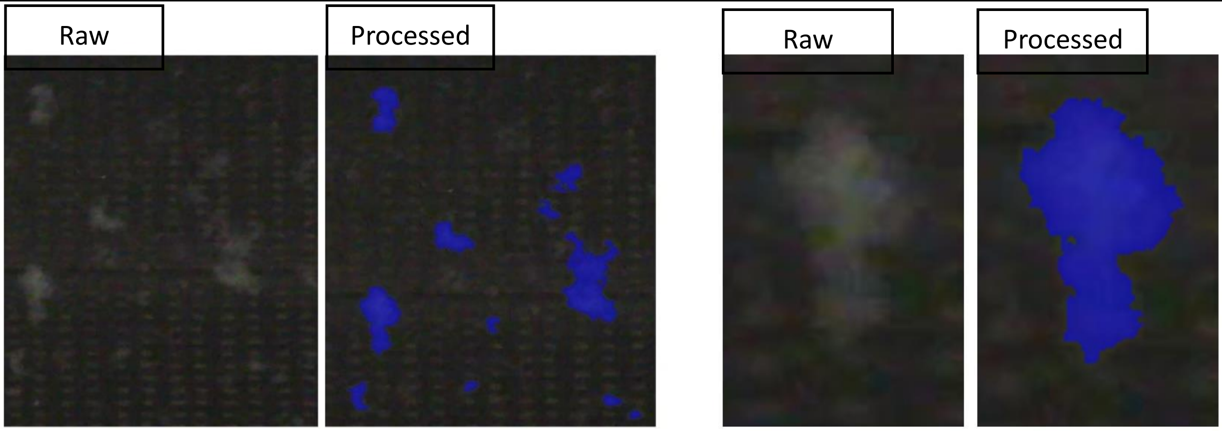

Figure 3.8. Image analysis of flocs

3.4.3. Application of D-optimal and RSM

The Response surface methodology was employed to examine different operational parameters. Design-Expert software version 13.0.0 integrates RSM techniques into its analysis methods, thereby simplifying expensive and complicated analyses. By merging statistical and mathematical approaches, RSM facilitates designers in evaluating the effectiveness of a variety of parameters. RSM consists of two fundamental principles: the identification of the optimal model and the assessment of the measured response.

A literature review led us to use optimal design as a modelling strategy in this study. As discussed in Chapter 1, both Central Composite Design and Box-Behnken Design were deemed unsuitable due to their inherent limitations, rendering them impractical for use in our research. The modeling of experiments consists of two main steps. Firstly, optimizing coagulant dosage and type under each condition; and secondly, optimizing polymer dosage and type under the same conditions.

During the initial step, a combination of three numerical factors and one categorical factor, each with varying levels, was utilized in an optimal design model to investigate the interaction between independent variables for phosphorus removal using alum and ferric coagulants. Each experiment was conducted independently under previously described conditions. To establish optimum conditions, a model was devised for analysis. To evaluate the effects of pH, temperature, coagulant dosage, and coagulant type on phosphorus removal, 90 experiments were carried out. Table 3.5 illustrates the independent variables and their levels.

Table 3.5. Matrix of optimal design (coagulation model)

Factor	Name	Units	Type	Minimum	Maximum	Range and level (coded)				
A	Coagulant dosage	mg/l	Numeric	32.40	129.60	-2 ↔ 32.40	-1 ↔ 48.6	0 ↔ 64.8	+1 ↔ 97.2	+2 ↔ 129.60
B	pH	-	Numeric	6.00	8.00	-	-1 ↔ 6.00	0 ↔ 7.00	+1 ↔ 8.00	-
C	Temperature	°C	Numeric	4.00	22.00	-	-1 ↔ 4.00	0 ↔ 12.00	+1 ↔ 22.0	-
D	Type of coagulant	-	Categoric	Ferric	Alum	-	-	-	-	-

For the second step, RSM with optimal design was utilized to explore the impact of different variables on phosphorus removal and generated sludge. A model was constructed to identify optimal conditions for analysis. To assess the impacts of pH, temperature, flocculant dosage, coagulant type, and type of flocculant on phosphorus removal, a total of 360 unique experiments with 3 replications for coagulation tests and 2 replications for flocculation tests were conducted.

Table 3.6. Matrix of optimal design (flocculation model)

Factor	Name	Units	Type	Minimum	Maximum	Range and level (coded)				
A	Flocculant dosage	mg/l	Numeric	4.10	27.10	-2 ↔ 4.1	-1 ↔ 6.8	0 ↔ 13.6	+1 ↔ 20.4	+2 ↔ 27.1
B	pH	-	Numeric	6.00	8.00	-	-1 ↔ 6.00	0 ↔ 7.00	+1 ↔ 8.00	-
C	Temperature	°C	Numeric	4.00	22.00	-	-1 ↔ 4.00	0 ↔ 12.00	+1 ↔ 22.0	-
D	Type of flocculant	-	Categoric	EM440CT	EM840MEB	-	-	-	-	-
E	Type of coagulant	-	Categoric	Ferric	Alum	-	-	-	-	-

3.5. Experimental Parameters

Each experiment was conducted within a controlled laboratory setting, where factors such as temperature, pH, camera position, mixing velocity, and environmental conditions were closely monitored and regulated to minimize any potential sources of error. The parameters governing the jar tests were precisely determined based on the guidelines outlined in the Laboratory Manual of Simplified Procedures for Water Examination (AWWA 1977). Moreover, prior to conducting the experiments, thorough calibrations and validations of equipment and instruments were performed to ensure their accuracy and reliability. This involved meticulous checks of pH meters, spectrophotometers, and other analytical tools used in the experimentation process. Additionally, strict adherence to safety protocols was maintained throughout the experiments to safeguard both the researchers and the integrity of the data. Personal protective equipment (PPE) such as lab coats, gloves, and goggles were worn at all times, and proper handling and disposal procedures were followed for any hazardous chemicals or waste generated during the experimentation process.

The experimental conditions employed in this study, have been documented and are presented in Table 3.5. This table provides a comprehensive overview of all parameters and variables controlled during the experiments.

Table 3.7. Experimental parameters

Parameter	Description
Wastewater sample	Altona Wastewater Treatment Facility
pH	6, 7, 8
Temperature	4 ±0.5 ºC, 12 ±0.5 ºC, 22 ±0.5 ºC
Type of coagulant	Alum, Ferric chloride
Coagulant dosage	(0, 32.4, 48.6, 64.8, 97.2, 129.6) mg/L
Type of flocculant	EM440CT, EM440MEB, EM840CT, EM840MEB
Flocculant dosage	(4.1, 6.8, 13.6, 20.4, 27.1) mg/L
Mixing conditions	130rpm for 5 minutes, 25rpm for 20 minutes
Imaging time	(0, 20, 40, 60, 140, 200, 300, 360) second
Analyzed parameter	Phosphorus, sludge weight
Image processing	Perimeter, Surface area
RSM	Optimal Design

3.6. Experimental Procedure

3.6.1. Jar Tests

In the following, a detailed explanation of the 2 stages involved in the experimental bench-scale tests is provided.

1. The temperature within the chamber was adjusted to the desired level, after which the wastewater sample was stored there for a period of 12 hours to allow it to stabilize.

2. With a manual stirrer, the wastewater sample contained within the 20-litre container was mixed in order to achieve uniform dispersion of particles.

3. The jar tester was positioned on its stand.

4. The pH of the sample was adjusted using 1 molar sodium hydroxide (NaOH) and 1 molar sulfuric acid (H_2SO_4) to the desired value.

5. using a 1000 ml graduated cylindrical beaker, a 1000 ml portion of the sample was dispensed into each square beaker.

6. During the first stage, coagulants were injected via syringes to determine the optimal dosage under varying conditions.

7. The motor of the stirrer was activated, and the mixing speed was set to 130 rpm for a duration of 5 minutes.

8. Subsequently, the stirring velocity was reduced to 25 rpm and continued for 20 minutes.

9. The stirring motor was then stopped, allowing the sample to settle for a period of 30 minutes.

10. Using a 30 ml pipette, samples of treated water were taken from the supernatant of each beaker.

11. Measurements of pH and phosphorus levels were recorded.

12. The experimentation process was repeated for different dosages, types of coagulants, or temperature variations as necessary.

In the second stage, identical procedures were followed, with the addition of applying a flocculant and measuring the weight of the sludge using the same method described previously.

1. The temperature within the chamber was adjusted to the desired level, after which the wastewater sample was stored there for a period of 12 hours to allow it to stabilize.

2. With a manual stirrer, the wastewater sample contained within the 20-litre container was agitated in order to achieve uniform dispersion of particles.

3. The jar tester was positioned on its stand.

4. The pH of the sample was adjusted to the desired value.

5. using a 1000 ml graduated cylindrical beaker, a 1000 ml portion of the sample was dispensed into each square beaker.

6. During the first stage, coagulants were injected via syringes to determine the optimal dosage under varying conditions.

7. The motor of the stirrer was activated, and the mixing speed was set to 130 rpm for a duration of 5 minutes.

8. 4 minutes after intense mixing, flocculant was injected into the wastewater using syringes.

8. The stirring velocity was reduced to 25 rpm and continued for 20 minutes.

9. The stirring motor was then stopped, allowing the sample to settle for a period of 30 minutes.

10. Using a 30 ml pipette, a sample of treated water was taken from the supernatant of each beaker.

11. Measurements of pH and phosphorus levels were recorded.

12. Following this, the supernatant was discharged, and the remaining sludge underwent filtration using a vacuum pump.

13. The filters were subsequently placed in an oven set at a temperature of 120 degrees Celsius for a duration of 12 hours.

14. The weight of the sludge was determined by subtracting the weight of the empty filter from the weight of the dried filter containing the sludge.

15. The experimentation process was repeated for different dosages, types of coagulants, types of flocculants, and temperature variations as necessary.

3.6.2. Image Capturing in the Laboratory

During the image-capturing phase, experimental tests were conducted on a bench-scale, with the entire process documented using a high-resolution camera. The experimental procedure has been detailed in previous sections. The following outlines the steps involved in image acquisition:

1. Positioning the camera and tripod in front of the square beaker, ensuring stability throughout the experiments.
2. Configuring optimal photography settings.
3. Establishing the connection between the camera and computer to regulate shutter parameters.

4. Capturing images of the black plate within the beaker to establish the pixel count associated with a specified standard length.
5. Taking photographs from the moment flocculant is injected until 360 seconds at intervals of 0, 20, 40, 60, 140, 200, 300, and 360 seconds.
6. Employing MATLAB for image processing.
7. Analyzing aggregate size and floc characteristics.
8. Repeating the test under different conditions.

Chapter 4. Results and Discussion

4.1. Overview

Two series of bench-scale experiments were conducted to investigate the optimal coagulant dosage in wastewater treatment under varying operational parameters.

In the initial phase, jar tests were performed at wastewater temperatures of 4°C, 12°C, and 22°C to evaluate the optimal coagulant dosage across different conditions. These conditions included the type of coagulant (Alum and Ferric), pH levels (6, 7, 8), and specific coagulant dosages (32.4mg/L, 48.6mg/L, 64.8mg/L, 97.2mg/L, and 129.6mg/L). The experimental design and conditions are summarized in Table 4.1. Subsequently, in the second phase of experiments, following the determination of optimal coagulant dosages under each set of conditions from the first series, a similar experimental setup was employed, adding two further operational variables. Specifically, the second phase introduced variations in the type of polymer used (EM44CT, EM840CT, EM440MEB, EM840MEB) and the dosage of flocculant (4.1mg/L, 6.8mg/L, 13.6mg/L, 20.4mg/L, 27.1mg/L) to explore treatment efficacy further. This expanded experimental design aimed to comprehensively assess the impact of coagulant and polymer dosages under a broader range of operating conditions.

Table 4.1. Experimental tests summary

Test run No	Temperature (°C)	pH	Coagulant type	Flocculant type	Coagulant dosage range (mg/L)	Flocculant dosage range (mg/L)
1	4, 12, 22	6, 7, 8	Alum	-	32.4 - 129.6	-
2	4, 12, 22	6, 7, 8	Ferric chloride	-	32.4 - 129.6	-
3	4, 12, 22	6, 7, 8	Alum	EM440CT	32.4 - 129.6	4.1 – 27.1
4	4, 12, 22	6, 7, 8	Ferric chloride	EM440MEB	32.4 - 129.6	4.1 – 27.1
5	4, 12, 22	6, 7, 8	Alum	EM840CT	32.4 - 129.6	4.1 – 27.1
6	4, 12, 22	6, 7, 8	Ferric chloride	EM840MEB	32.4 - 129.6	4.1 – 27.1

4.2. Response Surface Methodology

Statistical and mathematical models are employed to predict data that has not been explicitly provided. Despite potential variations in data quality within training sets, a robust and effective model is capable of accurately predicting outcomes. Failure to appropriately adjust models to training data can lead to overfitting, where a model becomes overly specific to the training data and exhibits a larger testing error compared to its training error. Overfitting occurs because the model has learned too many details from the training data, hindering its ability to generalize well to new, unseen data. To mitigate overfitting, cross-validation techniques are utilized during model development. Tables 4.2 and 4.3 present the experimental data and operating parameters for both the first and flocculation models, along with the corresponding actual and predicted responses.

Table 4.2. Optimal design matrix for RSM (coagulation model)

Run	**Coagulant Dosage (mg/L) (A)**	**pH (B)**	**Temperature (°C) (C)**	**Type of Coagulant (D)**	**Actual Phosphate (mg/L)**	**Predicted Phosphate (mg/L)**
1	64.80	7	12	Alum	0.361	0.370
2	97.20	8	22	Alum	0.790	0.730
3	32.40	6	22	Ferric	1.420	1.190
4	32.40	6	12	Alum	1.480	1.457
5	32.40	8	12	Alum	1.440	1.302
6	129.6	7	4	Alum	0.113	0.123
7	32.40	7	4	Ferric	1.140	1.107
8	129.6	7	22	Ferric	0.133	0.141
9	97.20	7	12	Ferric	0.170	0.128
10	129.6	7	4	Alum	0.113	0.123
11	129.6	6	4	Ferric	0.159	0.130
12	129.6	8	4	Ferric	0.132	0.135
13	32.40	6	12	Alum	1.480	1.457
14	64.80	8	12	Ferric	0.421	0.423
15	64.80	6	12	Ferric	0.271	0.380
16	64.80	7	22	Ferric	0.459	0.456
17	129.6	6	22	Alum	0.151	0.153
18	32.40	8	22	Ferric	1.690	1.984
19	97.20	8	22	Alum	0.790	0.730

Table 4.3. Optimal design matrix for RSM (flocculation model)

Run	Flocculant Dosage (mg/L) (A)	pH (B)	Temperature (°C) (C)	Type of Flocculant (D)	Type of Coagulant (E)	Actual Phosphate (mg/L)	Predicted Phosphate (mg/L)	Actual sludge weight (mg)	Predicted Sludge Weight (mg)
1	4.1	6	22	EM440CT	Alum	0.627	0.449	9.50	11.6
2	27.1	6	22	EM440CT	Ferric	0.197	0.356	17.1	14.7
3	13.6	8	22	EM440MEB	Ferric	0.000	0.000	43.7	46.4
4	27.1	7	4	EM440MEB	Alum	0.334	0.321	20.5	18.3
5	4.1	8	4	EM840CT	Ferric	1.050	0.959	15.9	15.2
6	13.6	8	22	EM440MEB	Ferric	0.000	0.000	43.7	46.40
7	4.1	7	22	EM840MEB	Ferric	0.198	0.201	28.1	35.2
8	20.4	7	22	EM840MEB	Ferric	0.404	0.295	26.1	21.2
9	27.1	6	22	EM840MEB	Alum	0.429	0469	11.2	11.8
10	6.8	6	22	EM440MEB	Alum	0.523	0.479	22.7	19.5
11	27.1	6	4	EM840CT	Ferric	0.477	0.438	20.0	19.4
12	27.1	7	4	EM440MEB	Alum	0.334	0.321	20.5	18.3
13	13.6	7	12	EM840CT	Ferric	0.912	0.782	12.6	13.0
14	6.8	8	4	EM840MEB	Alum	0.438	0.424	16.7	15.3
15	4.1	6	4	EM440CT	Ferric	0.357	0.355	17.2	15.8
16	20.4	7	4	EM440CT	Alum	0.315	0.470	17.7	18.1
17	4.1	6	22	EM840CT	Ferric	0.310	0.385	5.90	5.81
18	4.1	6	4	EM840CT	Alum	0.467	0.456	11.0	9.92
19	27.1	6	12	EM440CT	Alum	0.523	0.361	21.9	21.3
20	27.1	8	4	EM840CT	Alum	0.686	0.903	20.3	23.6
21	27.1	8	12	EM840MEB	Ferric	0.464	0.544	18.3	19.8
22	27.1	8	22	EM440CT	Alum	0.069	0.058	31.0	36.8
23	6.8	6	4	EM440MEB	Ferric	0.526	0.653	11.1	14.2
24	4.1	8	4	EM440MEB	Alum	0.636	0.545	13.3	13.2
25	27.1	8	22	EM840CT	Ferric	0.151	0.107	53.0	42.0
26	4.1	8	22	EM840CT	Alum	0.061	0.073	36.5	41.4
27	6.8	6	22	EM440MEB	Alum	0.523	0.479	22.7	21.9
28	13.6	6	4	EM840MEB	Ferric	0.570	0.474	10.1	12.1
29	4.1	8	22	EM440CT	Ferric	0.082	0.097	46.1	36.4
30	27.1	6	22	EM840CT	Alum	0.264	0.271	7.90	9.1
31	6.8	6	12	EM840MEB	Alum	0.370	0.475	16.8	13.4
32	4.1	7	12	EM440CT	Alum	0.586	0.682	15.5	18.1
33	27.1	6	22	EM440MEB	Ferric	0.168	0.162	16.4	19.9
34	27.1	8	4	EM440CT	Ferric	0.632	0.504	17.2	17.1

The reliability of the Response Surface Methodology (RSM) models can be assessed by examining the agreement between predicted and actual values of phosphate and sludge weight, as shown in Figure 4.1. In this figure, the experimental data points and corresponding model predictions are closely aligned along the normal line, indicating a strong correlation and consistency between observed and predicted values.

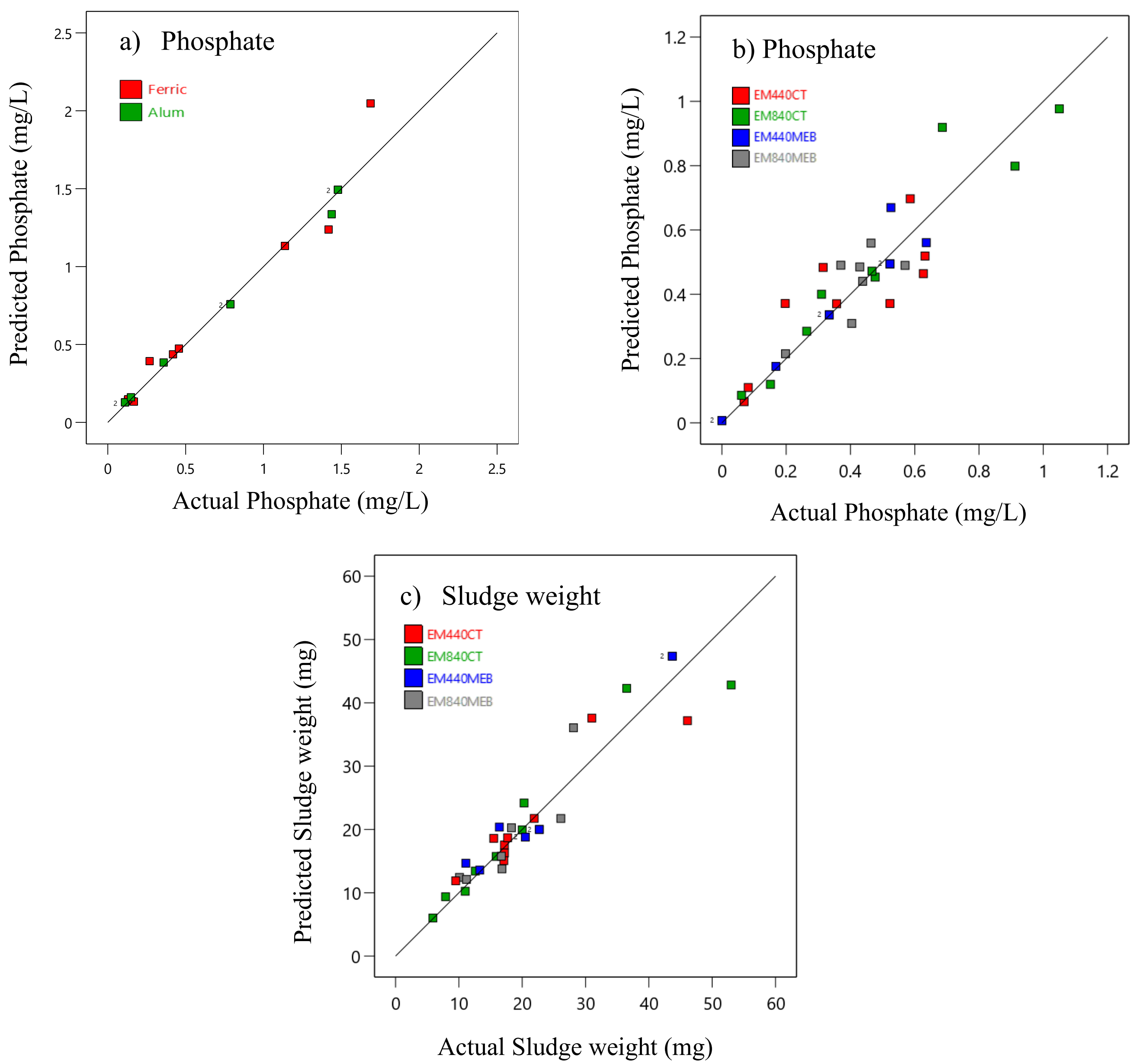

Figure 4.1. Optimal design predicted vs actual values for a) Phosphate (coagulation model), b)Phosphate (secod model), and c) Sludge weight (flocculation model)

4.2.1. Analysis of Variance (ANOVA)

To validate the model's significance, an Analysis of Variance (ANOVA) was conducted. ANOVA investigates how independent variables (factors) influence the dependent variables (Adelodun et al., 2019). The model is considered significant if the p-value is less than 0.05. Table 4.4 shows the performed ANOVA for both coagulation and flocculation models. Table 4.4 demonstrates that the models can predict the response with acceptable accuracy, indicating strong agreement between the predicted and experimentally obtained responses. The two indices, P-value and F-value, utilized in the modelling.

Table 4.4. ANOVA results

a) Phosphate

Source	Sum of Squares	Degree of Freedom	Mean Square	F-value	p-value
Model	1.07	10	0.1072	45.06	< 0.0001
R^2	0.9826	**Adjusted R^2**	0.9607		

b) Phosphate

Source	Sum of Squares	Degree of Freedom	Mean Square	F-value	p-value
Model	1.64	22	0.0744	6.30	< 0.0015
R^2	0.9264	**Adjusted R^2**	0.7793		

c) Sludge weight

Source	Sum of Squares	Degree of Freedom	Mean Square	F-value	p-value
Model	0.1428	22	0.0065	5.7	< 0.0024
R^2	0.9194	**Adjusted R^2**	0.7582		

4.2.2. Statistical Evaluation of Effects of Independent Variables

To assess the significant effects of independent variables such as temperature, pH, chemical dosage, and chemical type, an ANOVA was conducted. As mentioned earlier, a smaller p-value (<0.05) and a larger F-value indicate greater significance of that variable. The results of both models for examining model indices, significance of predictors, and reliability of predictions for all the linear, quadratic, and interaction effects of the studied factors are presented in Tables 4.5 and 4.6.

Table 4.5. Model statistical results for Phosphate (coagulation model)

Phosphate					
Source	**Sum of Squares**	**df**	**Mean Square**	**F-value**	**p-value**
Coagulant dosage	0.4774	1	0.4774	200.57	< 0.0001
pH	0.0130	1	0.0130	5.47	0.0475
Temperature	0.0068	1	0.0068	2.84	0.1302
Type of coagulant	0.0197	1	0.0197	8.28	0.0206
Coagulant dosage* pH	0.0125	1	0.0125	5.26	0.0509
Coagulant dosage* Temperature	0.0025	1	0.0025	1.04	0.3387
pH* Temperature	0.0265	1	0.0265	11.13	0.0103
Coagulant dosage* Coagulant dosage	0.0179	1	0.0179	7.51	0.0254
pH* pH	0.0225	1	0.0225	9.46	0.0152
Temperature* Temperature	0.0126	1	0.0126	5.28	0.0507

Table 4.6. a) Model statistical results for flocculation model (a) Phosphate, (b) sludge weight

Phosphate					
Source	**Sum of Squares**	**df**	**Mean Square**	**F-value**	**p-value**
Flocculant dosage	0.0407	1	0.0407	3.44	0.0904
pH	0.1611	1	0.1611	13.62	0.0036
Temperature	0.5568	1	0.5568	47.08	< 0.0001
Type of flocculant	0.0839	3	0.0280	2.36	0.1270
Type of coagulant	0.0104	1	0.0104	0.8794	0.3685
Flocculant dosage* pH	0.0053	1	0.0053	0.4508	0.5158
Flocculant dosage* Temperature	1.042E-06	1	1.042E-06	0.0001	0.9927
Flocculant dosage* Type of flocculant	0.0860	3	0.0287	2.42	0.1208
pH* Temperature	0.2872	1	0.2872	24.29	0.0005
pH* Type of flocculant	0.0997	3	0.0332	2.81	0.0889
Temperature* Type of flocculant	0.0435	3	0.0145	1.23	0.3461
Flocculant dosage* Flocculant dosage	0.0022	1	0.0022	0.1877	0.6732
pH*pH	0.0214	1	0.0214	1.81	0.2058
Temperature* Temperature	0.0321	1	0.0321	2.71	0.1278

Sludge weight					
Source	**Sum of Squares**	**df**	**Mean Square**	**F-value**	**p-value**
Flocculant dosage	0.0033	1	0.0033	2.88	0.1179
pH	0.0563	1	0.0563	49.45	< 0.0001
Temperature	0.0176	1	0.0176	15.42	0.0024
Type of flocculant	0.0071	3	0.0024	2.07	0.1629
Type of coagulant	0.0002	1	0.0002	0.1840	0.6763
Flocculant dosage*pH	0.0019	1	0.0019	1.65	0.2248
Flocculant dosage* Temperature	0.0023	1	0.0023	1.98	0.1865
Flocculant dosage* Type of flocculant	0.0065	3	0.0022	1.90	0.1885
pH* Temperature	0.0371	1	0.0371	32.55	0.0001
pH* Type of flocculant	0.0095	3	0.0032	2.77	0.0914
Temperature* Type of flocculant	0.0105	3	0.0035	3.06	0.0733
Flocculant dosage* Flocculant dosage	0.0010	1	0.0010	0.8934	0.3649
pH*pH	0.0002	1	0.0002	0.1448	0.7108
Temperature* Temperature	0.0002	1	0.0002	0.1496	0.7063

According to Table 4.5, the linear impacts of pH, coagulant concentration, and type on Phosphate removal are statistically significant, with p-values <0.0475, 0.0001 and 0.0206 respectively. Moreover, the interactive parameters such as between Temperature*pH and Coagulant dosage*pH significantly influence the response, with a p-value of 0.0103 and 0.050.9 (this value is so close to threshold 0.05 which means there is not strong enough evidence that this parameter has no effect on the response) indicating their importance. In addition, coagulant dosage is the most favorable significant model term with an F-ratio of 200.57. Conversely, interactions such as and Coagulant dosage*Temperature do not show a significant effect on Phosphate removal. In terms of quadratic effects, pH*pH and Temperature*Temperature and Coagulant dosage* Coagulant dosage are deemed highly significant, with P-values of 0.0152, 0.0507, and 0.0254 respectively.

For the flocculation model, Table 4.6, ANOVA results for Phosphate removal and sludge weight demonstrate that the linear coefficients of pH and temperature significantly affect the response. While other linear coefficients such as flocculant dosage, coagulant type and flocculant type are not significant. The only two-level interaction pH*Temperature is a significant model term with corresponding P-values of 0.0005, and 0.001 for Phosphate removal and sludge weight respectively. Additionally, all quadratic terms exhibit non-significant effects. Notably, the ANOVA results indicate that coefficients of significant effects have negative impacts on Phosphate removal and positive impacts on sludge weight.

4.2.3. Interaction Between Each Independent Variable and Response

4.2.3.1. Coagulation Model

The graphs in Figure 4.2 illustrate the correlation between the response variable (phosphate) and four independent variables: coagulant dosage, pH, temperature, and coagulant type. It is evident that increasing coagulant dosage positively impacts phosphate removal, leading to a decrease in phosphate concentration in the effluent. The phosphate levels have a quadratic relationship with pH. This means that the phosphate levels decrease to a minimum at 6.72 and then increase as pH moves from 6 to 8. Temperature is found to be insignificant variable with no observable effect on phosphate removal; however, the graphs indicate that optimal phosphate removal occurs at a temperature 11.48°C. Furthermore, concerning the type of coagulant, Ferric exhibits superior performance compared to Alum in terms of phosphate removal efficacy.

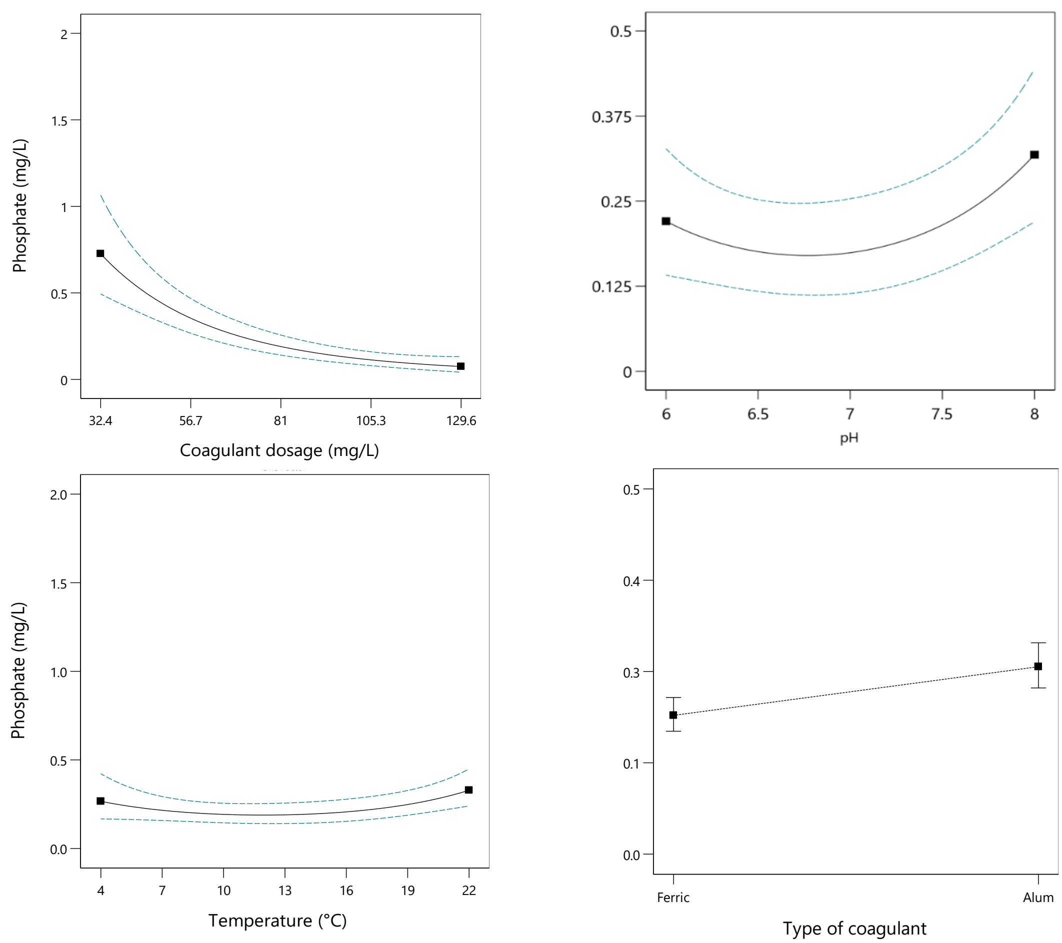

Figure 4.2. Effect of each factor on response (coagulation model)

4.2.3.2. Flocculation Model

Figure 4.3 shows the relationship between the response variable (phosphate) and four independent factors: flocculant dosage, pH, temperature, and flocculant type. Figure 5.2.a illustrates Increasing the flocculant dosage does not influence phosphate removal significantly, On the other hand, pH and temperature have a significant effect on phosphate removal and reduce phosphate concentration in the effluent. Figure 5.2.d also illustrates the influence of polymer type on phosphate removal. The graph indicates that the polymer with 40% cationic charge and lower molecular weight is more efficient compared to other polymers. Conversely, the polymer with 80% positive charge and higher molecular weight performed the worst in terms of phosphate removal efficacy. Lower molecular weight polymers typically exhibit higher reactivity due to their smaller size and greater surface area per unit mass. This increased reactivity enhances the polymer's ability to bind with phosphate ions, leading to more efficient removal.

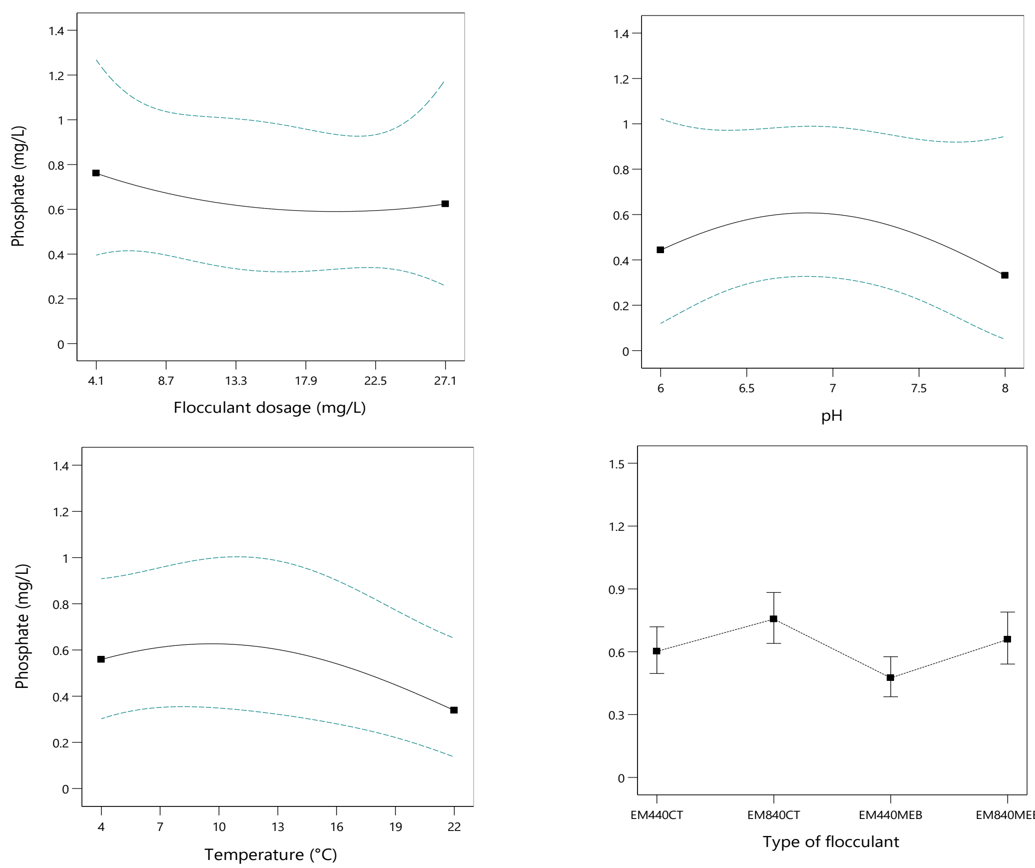

Figure 4.3. Effect of factors on phosphate removal (flocculation model)

Similarly, Figure 4.4 illustrates the relationship between sludge weight as the response variable and each independent factor. According to the ANOVA results and graphs 5.3.b and b, both pH and temperature are significant parameters that, when increased, lead to a slight increase in sludge weight. Conversely, flocculant dosage is deemed insignificant; however, increasing its concentration initially decreases sludge weight up to a certain amount before causing an increase.

Lastly, the polymer with 80% cationic charge and higher molecular weight produces less sludge, thereby making it easier to handle the generated sludge after coagulation.

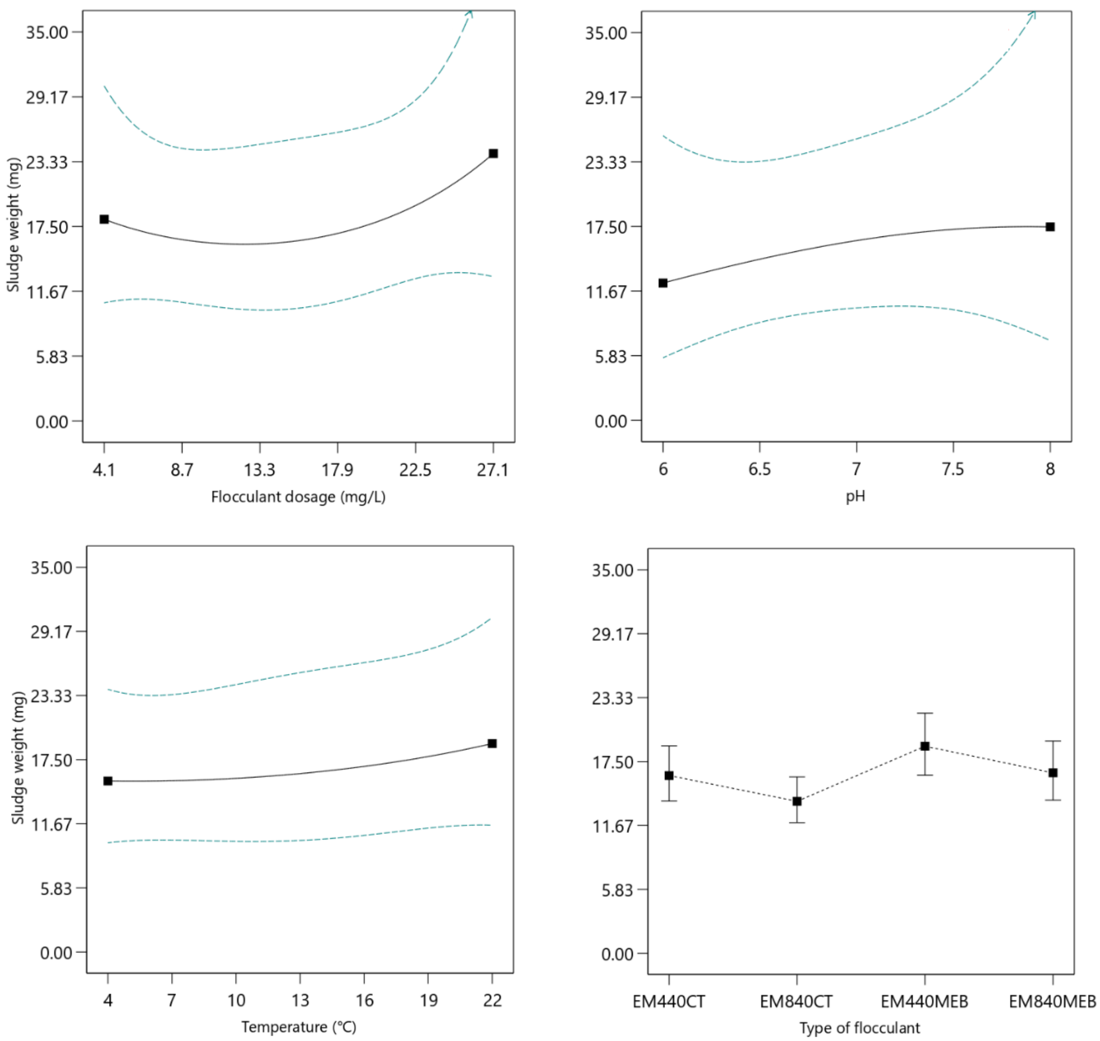

Figure 4.4. Effect of factors on sludge production (flocculation model)

4.2.4. Interaction Effect Between Input Independent Variables and Response (3D Plots)

3D graphs play a crucial role in visualizing and understanding the relationships between multiple independent variables and a response variable. These graphs allow researchers to identify optimal conditions for maximizing or minimizing the response variable. Peaks and valleys in the response surface indicate regions of high and low response values, respectively. By examining the 3D graph, one can pinpoint the combination of factor levels that optimize the response variable.

4.2.4.1 Coagulation Model

Figures 4.5.a and 4.5.b illustrate interactions involving temperature, Alum dosage, and phosphate, as well as interactions between Alum dosage, temperature and phosphate. As previously noted, temperature is not a significant factor and therefore does not notably influence phosphate levels. However, increasing coagulant dosageand pH leads to increased phosphate removal. Furthermore, Figure 4.5.c indicates a plateau-like result that higher phosphate removal occurs at extreme points of Temperature and pH. These graphs also demonstrate the specific conditions and optimal chemical amounts required to achieve phosphate levels of less than 1 mg/L.

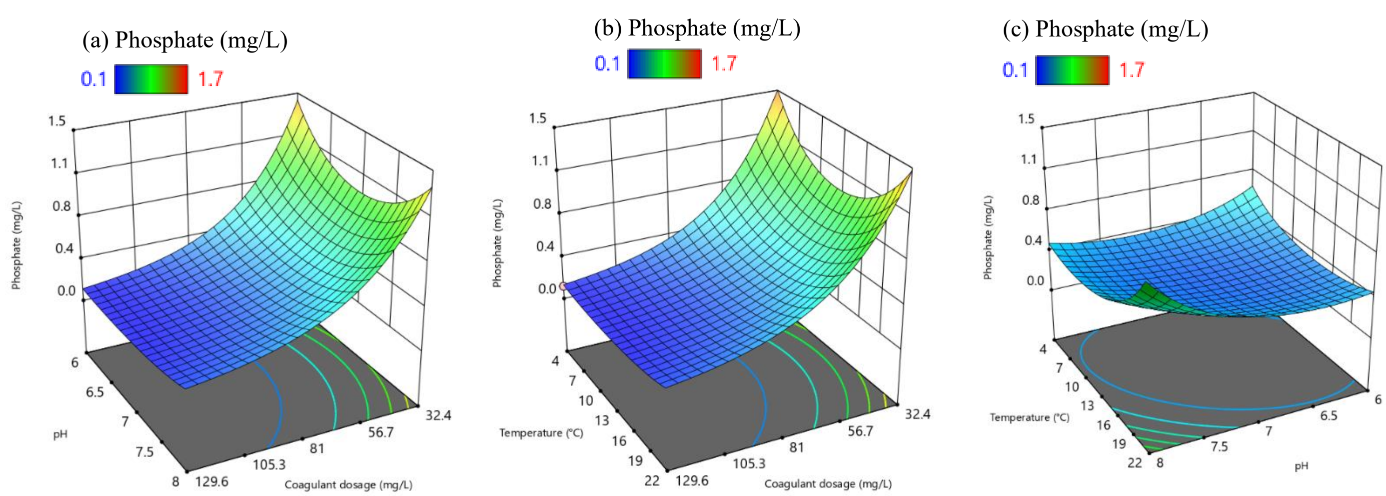

Figure 4.5. Interaction between independent factors and Phosphate removal (coagulant: Alum)

Similarly, comparable interactive results are observed when utilizing Ferric chloride as a coagulant. The findings from Figure 4.6, demonstrating enhanced phosphate removal compared to Alum.

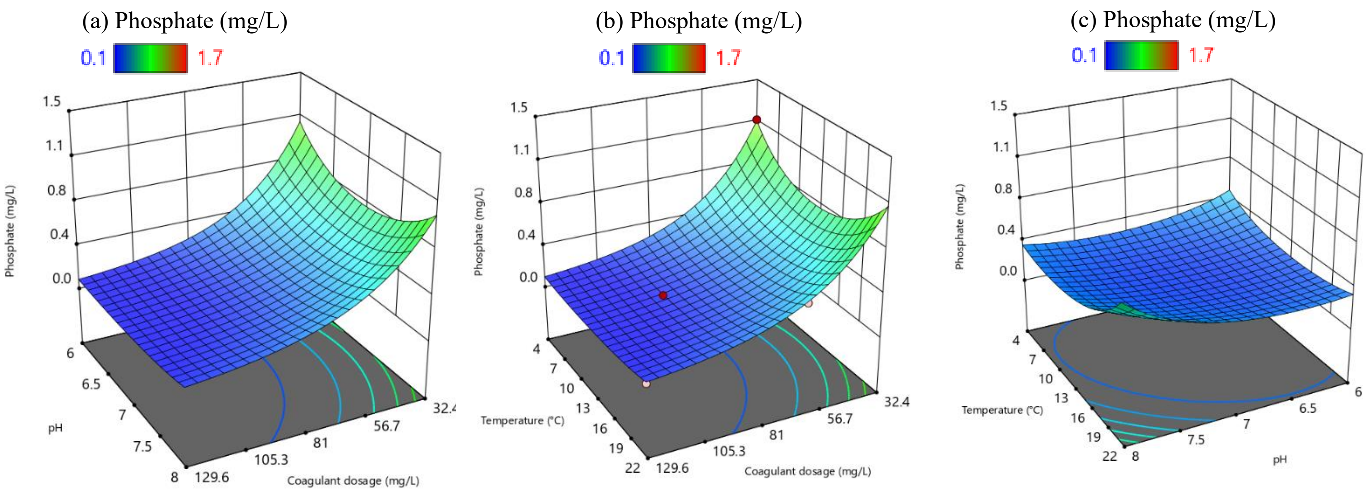

Figure 4.6. Interaction between independent factors and Phosphate removal (coagulant: Ferric)

4.2.4.2. Flocculation Model

Figure 4.7 presents an analysis of how phosphate responds to variations in key factors, including pH, temperature, and flocculant dosage.

a. pH and Flocculant Dosage: In Figure 4.7 a, the interaction between pH and flocculant dosage is explored. This analysis highlights the significant role of pH as a crucial factor influencing phosphate removal efficiency. The data from Figure 4.7.a indicates that higher phosphate removal rates are achieved at pH around 8. The plot also suggests that increasing flocculant dosage does not consistently improve phosphate removal, indicating a potential plateau effect or non-linear relationship between these variables.
b. Temperature and Flocculant Dosage: Figure 4.7.b focuses on the relationship between temperature, flocculant dosage, and phosphate removal. It reveals that higher temperatures are associated with more efficient phosphate removal. However, the impact of increasing flocculant dosage on removal rate appears to be minimal, suggesting that temperature plays

a more significant role in influencing phosphate removal under these experimental conditions.

c. pH and Temperature: In Figure 4.7.c, the combined effect of pH and temperature on phosphate removal is investigated. The findings demonstrate that higher temperatures coupled with elevated pH levels lead to the most efficient phosphate removal compared to other conditions. This highlights the importance of considering the interactive effects of pH and temperature when optimizing phosphate removal processes.

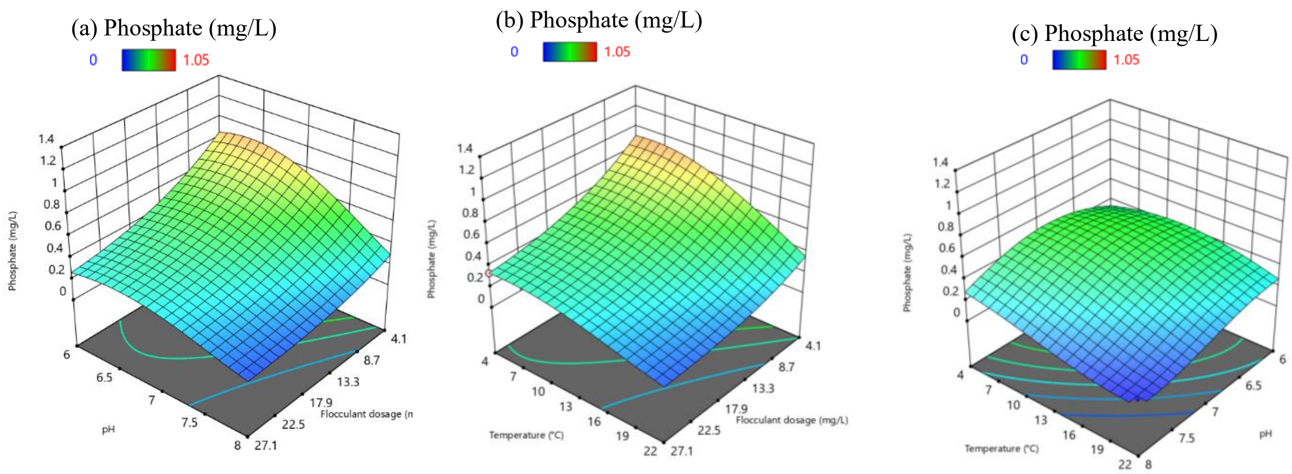

Figure 4.7. Interaction between independent factors and Phosphate removal (coagulant: Alum, flocculant: EM440MEB)

Similarly, Figure 4.8 illustrates the interaction between independent variables and the production of sludge as the response. These graphs provide insights into the conditions under which the amount of produced sludge can be minimized. By analyzing Figure 4.8, we can identify optimal operating conditions that result in reduced sludge production. The graphs reveal specific combinations of independent variables (such as pH, temperature, coagulant dosage, or polymer type) that lead to minimal sludge generation. It is obvious that lowering the flocculant dosage leads to a reduction in sludge production. This observation highlights the importance of optimizing flocculant usage to minimize sludge generation while maintaining effective water treatment. Additionally, lower pH levels are associated with less sludge production based on the trends observed in the graphs. This finding emphasizes the role of pH as a potential strategy for reducing sludge formation in water treatment systems. On the other hand, the graphs indicate that temperature does not have a significant effect on the amount of generated sludge under the studied conditions. This suggests that variations in temperature within the experimental range may not significantly impact sludge formation, highlighting pH and flocculant dosage as more influential factors in controlling sludge production.

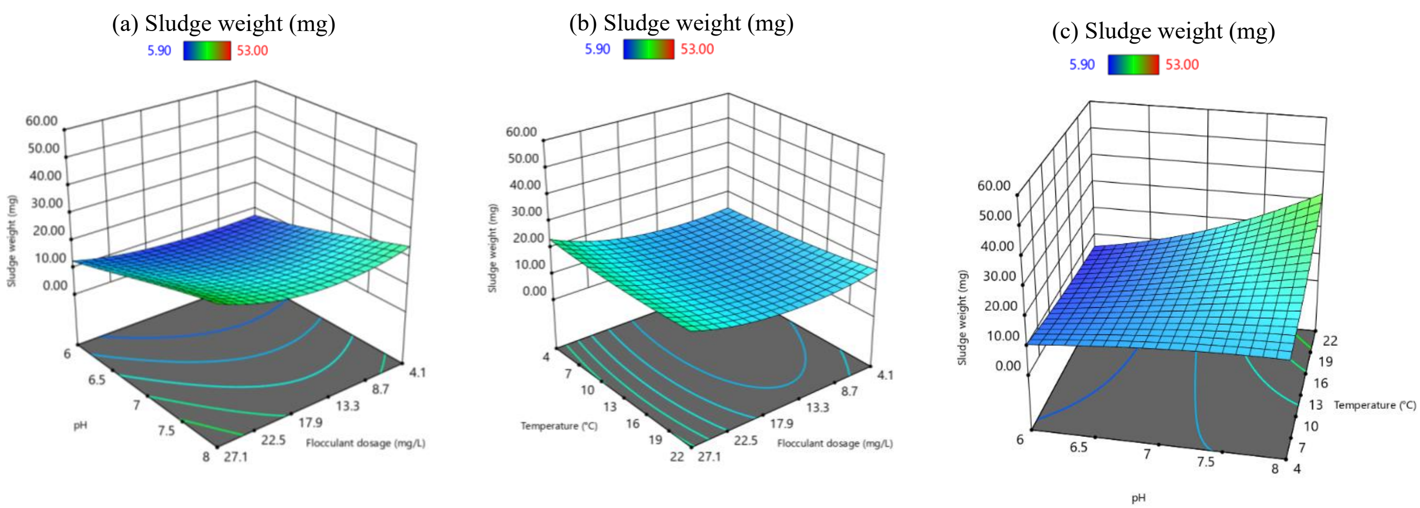

Figure 4.8. Interaction between independent factors and generated sludge (coagulant: Alum, flocculant: EM840CT)

4.2.5. Response Model Equations

The response surface regression model obtained through optimal design using Response Surface Methodology (RSM) presents equations with linear, quadratic, and interactive coefficients to predict responses (Y) for both models. Comparing the coefficients of the factors reveals their relative influence. The synergistic or antagonistic effects of the terms are determined by the positive or negative signs of their coefficients. Positive coefficients indicate synergy, while negative coefficients indicate antagonism. The linear model term Temperature for the Coagulation Model and Flocculant dosage, Flocculant concentration and coagulant type for the flocculation model, interactive terms including Coagulant dosage*pH, Coagulant dosage*Temperature, and quadratic term Temperature*Temperature for the Coagulation Model and terms Flocculation dosage, Flocculation type, Coagulation type, Flocculant dosage*pH, Flocculant dosage*Temperature, Flocculant dosage*Flocculant type, pH*Flocculant type, Temperature*Flocculant type, Dlocculant dosage*Flocculant dosage, pH*pH, and

Temperature*Temperature were identified insignificant effect on all responses. The equation in terms of coded factors can be used to make predictions about the response for given levels of each factor based on equations (1) to (3).

Coagulation model:

$(Y_{phosphate})$ ^ 0.3 = 0.6230 - 0.2627Coagulant dosage + 0.0372pH + 0.0357Coagulant type + 0.0729pH*Temperature + 0.1070 Coagulant dosage*Coagulant dosage + 0.0809pH*pH (4.1)

Flocculation model:

$(Y_{phosphate})$ ^ 0.44 = +0.7792 - 0.0774pH - 0.1512Temperature - 0.1330pH*Temperature (4.2)

$(Y_{sludge\ weight})$ ^ 0.1= +1.32 + 0.0398pH + 0.0283Temperature + 0.0478pH*Temperature (4.3)

4.2.6. Phosphate Removal and Sludge Generated Optimization

In order to optimize the removal of phosphate and generated sludge, the input parameters including type of coagulant, type of flocculant, flocculant dosage, temperature, and pH were adjusted to operate within optimal conditions. Using numerical optimization techniques, 100 experimental solutions were generated with a desirability ranging from 76.7% to 85.2%.

In the ramp figure displayed in Figure 5.8, the best optimal response was identified for specific input conditions:

- Flocculant dosage = 4.1 mg/L

- pH = 6.59

- Temperature = 8.56°C

- Type of flocculant = within specified range

- Type of coagulant = within specified range

This optimal configuration achieved a desirability rating of 85.2%, resulting in a phosphate level of 0.916 mg/L and a sludge weight of 11.65 mg.

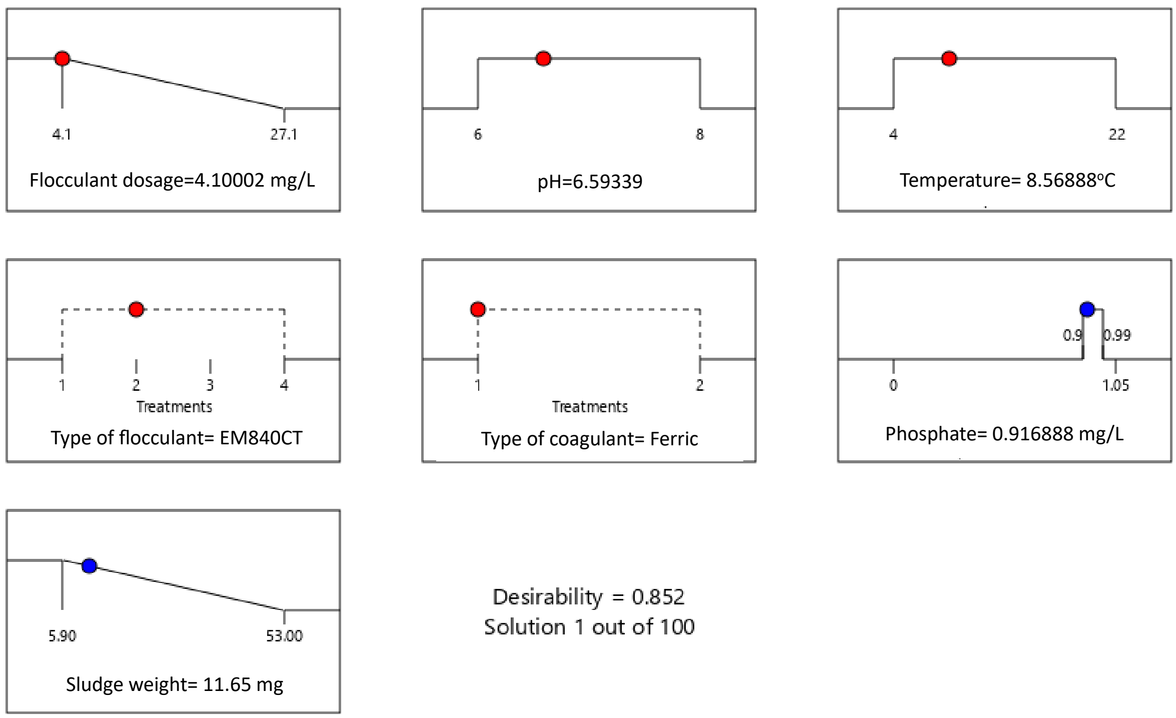

Figure 4.9. Ramp plot using the numerical technique for optimal conditions

4.3. Artificial Neural Network Model

Python 3.12.3 was utilized to develop and train an Artificial Neural Network (ANN) model using the functions and tools available in Python's library. Throughout this study, different data partitions and various configurations of hidden layers with varying numbers of neurons were explored to determine the optimal model. After several iterations, a decision was made to allocate 85% of the data for training the model and reserve 15% for testing.

The trained ANN model is illustrated in Figure 4.10 and is structured as a three-layered back-propagation neural network. In order to minimize prediction error the model design was determined to include one hidden layer with 21 neurons, one input with 9 neurons and one output layer with 1 neuron.

Hidden Layer

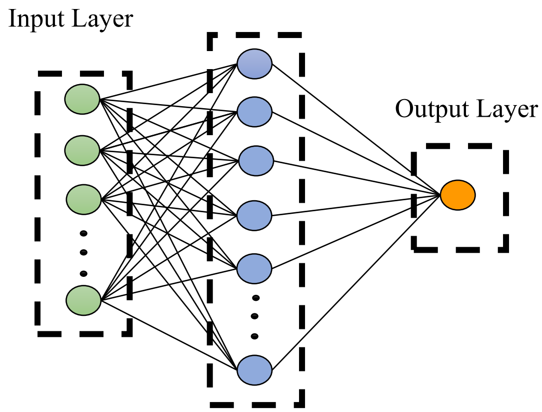

Figure 4.10. Artificial neural network training model with hidden layer and number of neurons

Given the non-linear nature of the data, the rectified linear unit (ReLU) activation function was employed during model training, and the Adam optimizer was selected as the solver. The activation function in the hidden layer transforms the input into a format recognizable by the output layer.

The R-squared (R) values obtained for both the Phosphate level and sludge weight testing sets are values of 0.7994 and 0.7965, respectively (as shown in Figure 4.11). Additionally, the Mean Squared Error (MSE) for the testing set is 0.0102 and 25.8664, respectively. These values indicate strong model performance, with lower MSE values and higher R-squared values providing further validation of the model's accuracy.

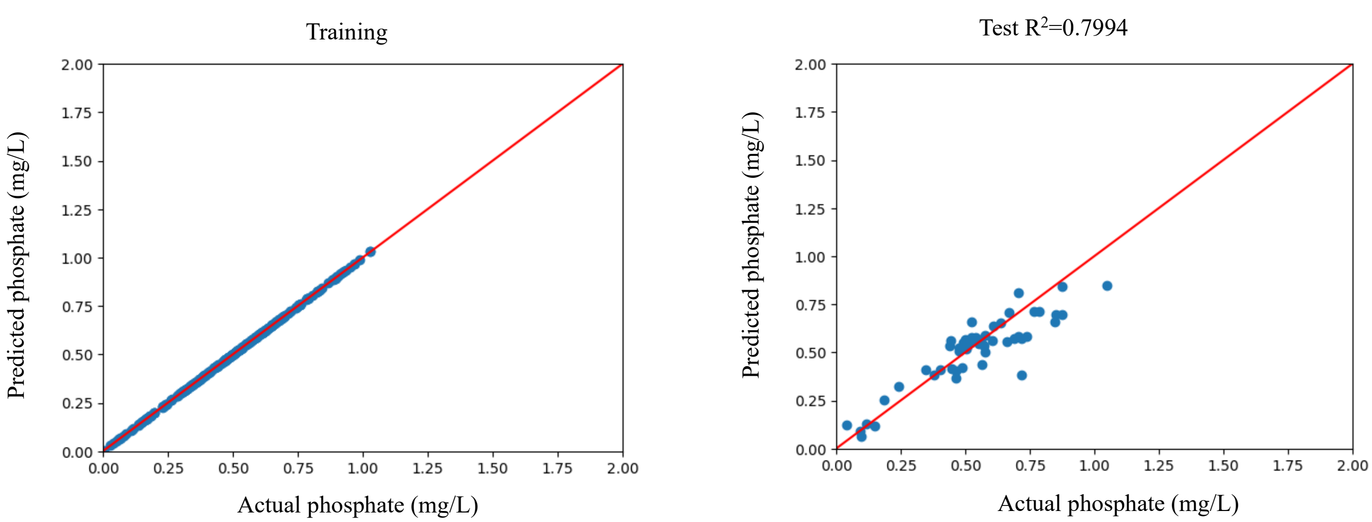

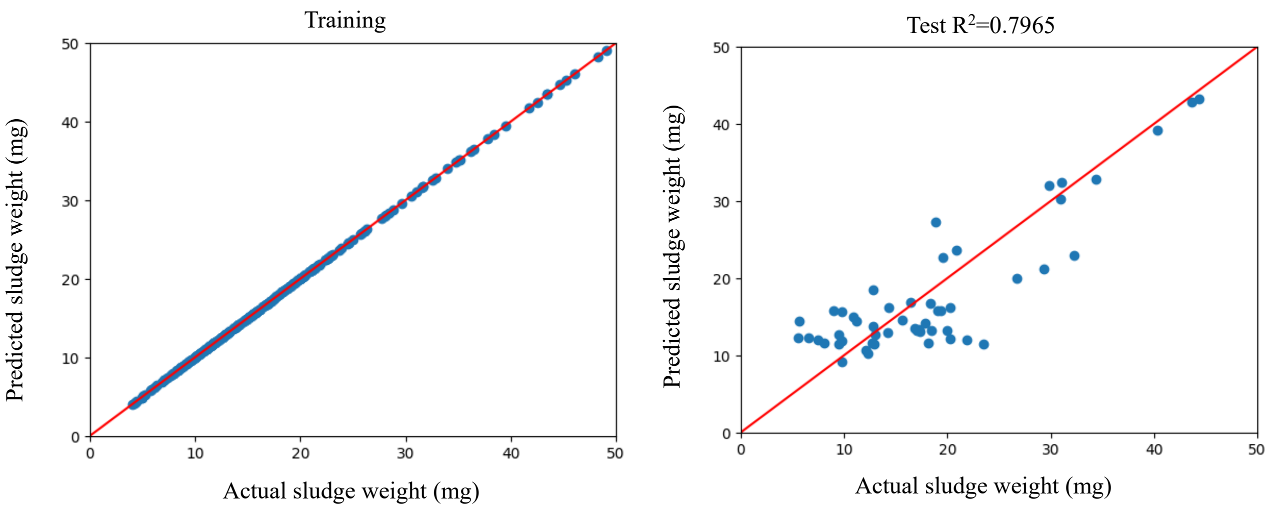

Figure 4.11. Regression analysis for ANN model

4.4. Validating of the Models

In order to compare the results of the RSM, ANN, and experimental tests, 10 random experiments were selected (Figure 4.12). The selection aimed to evaluate the predictive performance of the Response Surface Methodology (RSM) and Artificial Neural Networks (ANN) against actual experimental outcomes.

As illustrated in Figure 4.12, the comparative analysis reveals that the Artificial Neural Network (ANN) outperforms the Response Surface Methodology (RSM) in accurately predicting the final phosphate level. Specifically, the phosphate concentrations obtained through RSM, ANN, and experimental tests are 0.382, 0.331, and 0.377, respectively. This indicates that the ANN model provides a more precise estimation of the phosphate levels compared to the RSM approach.

On the other hand, Both ANN and RSM model demonstrates significant predictive capability in estimating the weight of generated sludge, showing a notable agreement with the experimental results. The respective values obtained for RSM, ANN, and experimental tests regarding the weight of generated sludge are 22.6, 16.2, and 20.3.

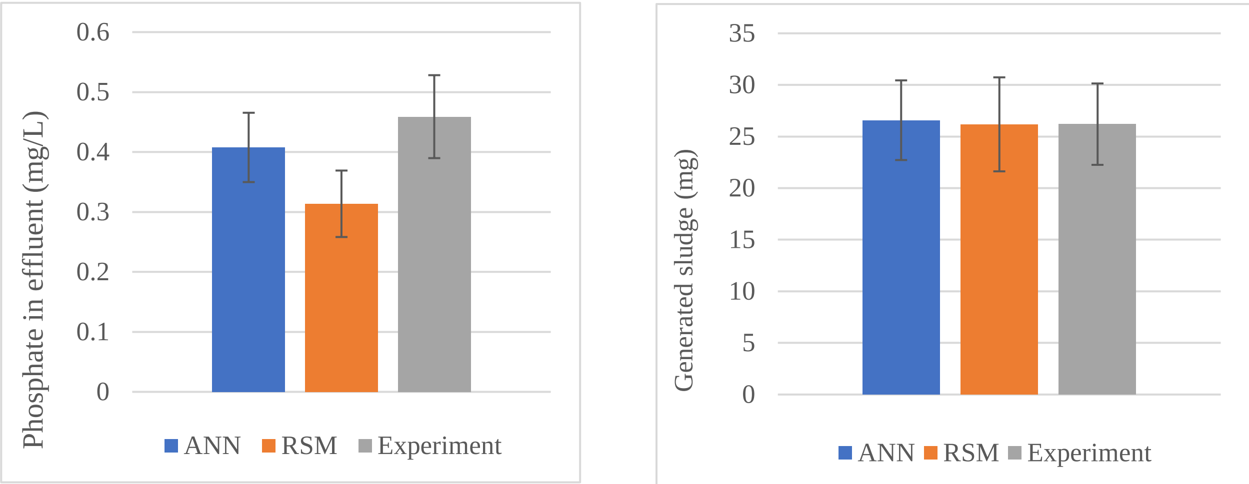

Figure 4.12. Validation results for RSM, ANN, and experimental test for phosphate removal at coagulant

Chapter 5: Conclusion

Based on the experimental tests, mathematical and statistical models, and the use of a digital camera for capturing flocs in this study, we developed two models to predict the final phosphate concentration in the effluent.

1. Experiments were carried out across diverse conditions, yielding extensive data for analysis. The coagulation model, which focused on optimizing coagulant dosage, underscored the pivotal role of coagulants in wastewater chemical treatment. It was observed that increasing coagulant dosage enhances process efficiency. However, exceeding a dosage of 105.3 mg/l for Alum and ferric chloride did not yield significant improvements in removal rates. On the other hand, variations in temperature and pH were found to have minimal impact on phosphate removal efficiency. Optimal removal was observed at approximately pH 7 and temperatures around 13 degrees Celsius.
2. The flocculation model focused on optimizing phosphate removal and sludge weight under identical conditions with adding coagulation aid. The incorporation of a flocculant altered the dynamics of previously analyzed factors in terms of phosphate removal. While increasing the dosage of flocculant (polymer dosage) was observed to have a negligible impact on the treatment process, analysis through image processing revealed that overdosing could have adverse effects on flocculation, resulting in the formation of smaller flocs.

   Temperature emerged as a critical factor influencing flocculation. Lower temperatures were associated with reduced phosphate removal rates, while higher temperatures facilitated enhanced flocculation, thereby improving the treatment efficiency.

   A notable finding from the experiments pertained to the influence of pH on phosphate removal. It was observed that at neutral pH levels, phosphate removal was notably inadequate. However, at pH 6 and particularly at pH 8, phosphate removal rates were significantly higher, indicating the effect of pH on the efficiency of phosphate removal.

   When considering the efficiency of polymers in flocculation, the optimal molecular weight and cationic charge depend on various factors such as the specific characteristics of the wastewater, the concentration of suspended solids, and the desired treatment objectives. While heavy polymers (those with relatively high molecular weights) are generally effective in promoting flocculation by forming strong bridges between particles, there is a point beyond which increasing molecular weight may not necessarily lead to further improvement in flocculation efficiency. Very heavy polymers, often characterized by extremely high molecular weights, can sometimes exhibit diminished efficiency in flocculation. This can occur due to several reasons:

a. Hindered mobility: Very heavy polymers may have reduced mobility in solution, making it more challenging for them to effectively interact with suspended particles and promote flocculation.

b. Increased viscosity: Extremely high molecular weight polymers can lead to significantly higher solution viscosities, which may hinder the dispersion of the polymer throughout the wastewater and reduce the formation of flocs.

c. Shear sensitivity: Very heavy polymers may be more susceptible to degradation under high shear conditions, such as those encountered during mixing or pumping processes, which can diminish their effectiveness in flocculation.

3. Regarding sludge weight, increasing the dosage of flocculant has a negative impact, resulting in challenges associated with handling the generated sludge post-treatment. Exceeding a dosage of 13.3 mg/l of polymer contributes to increased sludge production. Additionally, elevating the pH from 6 to 8 and the temperature from 4 to 22 degrees Celsius similarly results in higher quantities of generated sludge.
4. This research employed Artificial Neural Networks (ANN) to forecast the final phosphate in effluent and generated sludge. By optimizing the inputs (flocs perimeter, flocs projected area, temperature, pH, coagulant dosage, flocculant dosage, time, coagulant type, flocculant type), two water quality variables (effluent concentrations of phosphate and quantity of sludge) were selected as outputs to construct the ANN model. The results showed that a model with one hidden layer with 21 neurons is able to obtain the R-squared (R^2) values for both the Phosphate level and sludge weight at 0.7994 and 0.7965, respectively.

Chapter 6: Engineering Significance

6.1. Significance

Numerous endeavours have been undertaken to provide statistical models capable of predicting outputs based on input variables. This study successfully developed models that could potentially be integrated into online sensors for predicting phosphate levels and generated sludge in effluent. The research effectively achieved its primary objectives of creating models for predicting phosphate levels in effluent and estimating the quantity of generated sludge. A comprehensive analysis of operational factors was conducted using Response Surface Methodology (RSM). Furthermore, the fractal perimeter and area of coagulation/flocculation flocs were directly determined from images, facilitated by the application of a high-speed camera with appropriate image resolution. The results obtained were in line with major trends observed in previous studies on similar aggregates. The research highlighted that any alteration in coagulation/flocculation processes, such as the addition of polymers, can influence the impact of operational parameters on wastewater treatment. Notably, the investigation involved the direct analysis of flocs from real chemical treatment processes in an environmental laboratory, enabling a direct correlation of results with practical challenges encountered in water treatment plants.

6.2. Recommendation For Future Studies

This research focused on the development of two statistical models aimed at predicting specific desired outputs. The findings suggest a potential for the further advancement of two online sensor prototypes, leveraging Response Surface Methodology (RSM) and Artificial Neural Networks (ANN), to facilitate real-time measurement of phosphate levels in wastewater treatment plants. Specialized software tailored to these operations would be essential for successful implementation.

To enhance the accuracy of the models, the utilization of super high-resolution cameras for capturing images of flocs could be instrumental. This approach holds promise for improving the precision of the ANN model through enhanced image analysis capabilities.

Preliminary tests were conducted with anionic, neutral, and cationic polymers, leading to the decision to employ current positively charged polymers in this study. It is advisable to explore the use of very low positively charged polymers to analyze differences between them and high and very high cationic polymers. Additionally, incorporating other organic coagulants alongside these polymers could potentially enhance the treatment process and reduce chemical consumption, thereby optimizing overall efficiency.

Furthermore, in the model-building process, two outputs were utilized. It is recommended to expand the number of outputs to include parameters such as turbidity, Total Suspended Solids (TSS), and color to evaluate the performance of these models with the incorporation of additional outputs. This approach would provide a more comprehensive understanding of the models' effectiveness across various treatment parameters.

References:

AlGhazzawi, A., & Lennox, B. (2009). Model predictive control monitoring using multivariate statistics. Journal of Process Control, 19(2), 314–327. https://doi.org/10.1016/J.JPROCONT.2008.03.007

Alves, M., Cavaleiro, A. J., Ferreira, E. C., Amaral, A. L., Mota, M., Da Motta, M., Vivier, H., & Pons, M.-N. (2000). Characterisation by image analysis of anaerobic sludge under shock conditions.

Amaral, A. L., & Ferreira, E. C. (2005). Activated sludge monitoring of a wastewater treatment plant using image analysis and partial least squares regression. Analytica Chimica Acta, 544(1–2), 246–253. https://doi.org/10.1016/J.ACA.2004.12.061

American Water Works Association, & American Society of Civil Engineers. (2012). Water Treatment Plant Design 5/E (5th ed.).

Amirtharajah, A., & Mills, K. M. (1982). Rapid-mix design for mechanisms of alum coagulation. Journal American Water Works Association, 74(4), 210–216. https://doi.org/10.1002/J.1551-8833.1982.TB04890.X

Asadi-Ghalhari, M., Usefi, S., Ghafouri, N., Kishipour, A., Mostafaloo, R., & Tabatabaei, F. sadat. (2023). Modeling and optimization of the coagulation/flocculation process in turbidity removal from water using poly aluminum chloride and rice starch as a natural coagulant aid. Environmental Monitoring and Assessment, 195(4), 1–11. https://doi.org/10.1007/S10661-023-11150-8/METRICS

Bache, D. H., & Gregory, R. (2007). Flocs in Water Treatment. Water Intelligence Online, 6(0), 9781780402000–9781780402000. https://doi.org/10.2166/9781780402000

Benalia, A., Baatache, O., Derbal, K., Khalfaoui, A., Amrouci, Z., Pizzi, A., & Panico, A. (2024). The use of central composite design (CCD) to optimize and model the coagulation-flocculation process using a natural coagulant: Application in jar test and semi-industrial scale. Journal of Water Process Engineering, 57, 104704. https://doi.org/10.1016/J.JWPE.2023.104704

Bi, J., Chen, Z., Yuan, H., & Zhang, J. (2024). Accurate water quality prediction with attention-based bidirectional LSTM and encoder–decoder. Expert Systems with Applications, 238, 121807. https://doi.org/10.1016/J.ESWA.2023.121807

Boisvert, J. P., To, T. C., Berrak, A., & Jolicoeur, C. (1997). Phosphate adsorption in flocculation processes of aluminium sulphate and poly-aluminium-silicate-sulphate. Water Research, 31(8), 1939–1946. https://doi.org/10.1016/S0043-1354(97)00042-0

Bourcier, D., Féraud, J. P., Colson, D., Mandrick, K., Ode, D., Brackx, E., & Puel, F. (2016). Influence of particle size and shape properties on cake resistance and compressibility during pressure filtration. Chemical Engineering Science, 144, 176–187. https://doi.org/10.1016/J.CES.2016.01.023

Box, G. E. P., & Wilson, K. B. (1992). On the Experimental Attainment of Optimum Conditions. 270–310. https://doi.org/10.1007/978-1-4612-4380-9_23

Bratby, J. (2016). Coagulation and Flocculation in Water and Wastewater Treatment – Third Edition. Water 21, AUG., 25–27. https://doi.org/10.2166/9781780407500

Brij M. Moudgil, & Bernard J. Scheiner. (1988). Flocculation and Dewatering.

Chakraborti, R. K., Gardner, K. H., Atkinson, J. F., & Van Benschoten, J. E. (2003). Changes in fractal dimension during aggregation. Water Research, 37(4), 873–883. https://doi.org/10.1016/S0043-1354(02)00379-2

Chemicals / Process optimization - AMCON Europe s.r.o. (n.d.). Retrieved March 6, 2024, from https://www.amcon-eu.com/chemicals-process-optimization/

Chen, C. L., & Hou, P. L. (2006). Fuzzy model identification and control system design for coagulation chemical dosing of potable water. Water Science and Technology: Water Supply, 6(3), 97–104. https://doi.org/10.2166/WS.2006.782

Coufort, C., Dumas, C., Bouyer, D., & Liné, A. (2008). Analysis of floc size distributions in a mixing tank. Chemical Engineering and Processing, 47(3), 287–294. https://doi.org/10.1016/J.CEP.2007.01.009

Da Motta, M., Pons, M. N., Roche, N., & Vivier, H. (2001). Characterisation of activated sludge by automated image analysis. Biochemical Engineering Journal, 9(3), 165–173. https://doi.org/10.1016/S1369-703X(01)00138-3

Dagot, C., Pons, M. N., Casellas, M., Guibaud, G., Dollet, P., & Baudu, M. (2001). Use of image analysis and rheological studies for the control of settleability of filamentous bacteria: Application in SBR reactor. Water Science and Technology, 43(3), 27–33. https://doi.org/10.2166/WST.2001.0115

Dai, H., Qiu, Z., Hu, F., Gao, C., Chen, Y. F., & Zhou, Z. (2019). Floc Performance parameters during water treatment in a micro-vortex flocculation process determined by machine vision. Environmental Technology, 40(23), 3062–3071. https://doi.org/10.1080/09593330.2018.1465127

Daud, N. M., Sheikh Abdullah, S. R., & Abu Hasan, H. (2018). Response surface methodological analysis for the optimization of acid-catalyzed transesterification biodiesel wastewater pre-treatment using coagulation–flocculation process. Process Safety and Environmental Protection, 113, 184–192. https://doi.org/10.1016/J.PSEP.2017.10.006

Deniz, V. (2015). Dewatering of barite clay wastewater by inorganic coagulants and co-polymer flocculants. Physicochemical Problems of Mineral Processing, 51(1), 351–364. https://doi.org/10.5277/PPMP150131

Diamadopoulos, E., & Vlachos, C. (1996). Coagulation-filtration of a secondary effluent by means of pre-hydrolyzed coagulants. Water Science and Technology, 33(10–11), 193–201. https://doi.org/10.1016/0273-1223(96)00420-9

Douglas C. Montgomery. (2008). Design and Analysis of Experiments (7th ed., pp. 0–680).

Edzwald, J. K. (2013). Coagulant mixing revisited: Theory and practice. Journal of Water Supply: Research and Technology - AQUA, 62(2), 67–77. https://doi.org/10.2166/AQUA.2013.142

El-taweel, R. M., Mohamed, N., Alrefaey, K. A., Husien, S., Abdel-Aziz, A. B., Salim, A. I., Mostafa, N. G., Said, L. A., Fahim, I. S., & Radwan, A. G. (2023). A review of coagulation explaining its definition, mechanism, coagulant types, and optimization models; RSM, and ANN. In Current Research in Green and Sustainable Chemistry (Vol. 6). Elsevier B.V. https://doi.org/10.1016/j.crgsc.2023.100358

Fettig, J., Ratnaweera, H. C., & Ødegaard, H. (1990). Simultaneous Phosphate Precipitation and Particle Destabilization Using Aluminium Coagulants of Different Basicity. Chemical Water and Wastewater Treatment, 221–242. https://doi.org/10.1007/978-3-642-76093-8_15

Fitzpatrick, C. S. B., Fradin, E., & Gregory, J. (2004). Temperature effects on flocculation, using different coagulants. Water Science and Technology, 50(12), 171–175. https://doi.org/10.2166/WST.2004.0710

Franceschi, M., Girou, A., Carro-Diaz, A. M., Maurette, M. T., & Puech-Costes, E. (2002a). Optimisation of the coagulation–flocculation process of raw water by optimal design method. Water Research, 36(14), 3561–3572. https://doi.org/10.1016/S0043-1354(02)00066-0

Franceschi, M., Girou, A., Carro-Diaz, A. M., Maurette, M. T., & Puech-Costes, E. (2002b). Optimisation of the coagulation–flocculation process of raw water by optimal design method. Water Research, 36(14), 3561–3572. https://doi.org/10.1016/S0043-1354(02)00066-0

Ganczarczyk, J. J., & Rizzi, M. (1996). Mechanism of sludge formation and dewatering. Proceedings of the CSCE 4th Environmental Engineering Conference, Edmonton, AT, May 29-1 June.

Gholami, M., Ghaneian, M. T., Fatemi, S. S., Talebi, P., & Dalvand, A. (2022). Investigating the efficiency of coagulation and flocculation process in wastewater treatment of paper and cardboard recycling industry. International Journal of Environmental Analytical Chemistry, 102(17), 5860–5872. https://doi.org/10.1080/03067319.2020.1804891

Global Coagulant Market Size and Forecast to 2030. (n.d.). Retrieved March 6, 2024, from https://www.skyquestt.com/report/coagulant-market

Gorczyca, B., & Ganczarczyk, J. (1996). Image Analysis of Alum Coagulated Mineral Suspensions. Environmental Technology, 17(12), 1361–1369. https://doi.org/10.1080/09593331708616505

Gorczyca, B., & Ganczarczyk, J. (1999). Structure and Porosity of Alum Coagulation Flocs. Water Quality Research Journal, 34(4), 653–666. https://doi.org/10.2166/WQRJ.1999.034

Gorczyca, B., & Klassen, P. (2008). Optimization of Solids Separation in Dissolved Air Flotation. Water Quality Research Journal, 43(2–3), 239–247. https://doi.org/10.2166/WQRJ.2008.027

Gregory, J. (1978). Effects of Polymers on Colloid Stability. The Scientific Basis of Flocculation, 101–130. https://doi.org/10.1007/978-94-009-9938-1_6

He, W., Nan, J., Li, H., & Li, S. (2012). Characteristic analysis on temporal evolution of floc size and structure in low-shear flow. Water Research, 46(2), 509–520. https://doi.org/10.1016/J.WATRES.2011.11.040

Henderson, J. M., & Wheatley, A. D. (1987). Factors affecting a loss of flocculation activity of polyacrylamide solutions: Shear degradation, cation complexation, and solution aging. Journal of Applied Polymer Science, 33(2), 669–684. https://doi.org/10.1002/APP.1987.070330228

Hilligardt, D., & Hoffmann, E. (1997). Particle size analysis and sedimentation properties of activated sludge flocs. Water Science and Technology, 36(4), 167–175. https://doi.org/10.1016/S0273-1223(97)00436-8

Hjorth, M., & Jørgensen, B. U. (2012). Polymer flocculation mechanism in animal slurry established by charge neutralization. Water Research, 46(4), 1045–1051. https://doi.org/10.1016/J.WATRES.2011.11.078

Jiang, J.-Q., & Graham, N. (1998a). Pre-polymerised inorganic coagulants and phosphorus removal by coagulation - A review. Water SA.

Jiang, J.-Q., & Graham, N. (1998b). Pre-polymerised inorganic coagulants and phosphorus removal by coagulation - A review. Water SA.

Jin, Y. (2005). USE OF A HIGH RESOLUTION PHOTOGRAPHIC TECHNIQUE FOR STUDYING COAGULATION/FLOCCULATION IN WATER TREATMENT.

Joo, D. S., Choi, D. J., & Park, H. (2000). The effects of data preprocessing in the determination of coagulant dosing rate. Water Research, 34(13), 3295–3302. https://doi.org/10.1016/S0043-1354(00)00067-1

Jorfi, S., Barzegar, G., Ahmadi, M., Darvishi Cheshmeh Soltani, R., Alah Jafarzadeh Haghighifard, N., Takdastan, A., Saeedi, R., & Abtahi, M. (2016). Enhanced coagulation-photocatalytic treatment of Acid red 73 dye and real textile wastewater using UVA/synthesized MgO nanoparticles. Journal of Environmental Management, 177, 111–118. https://doi.org/10.1016/J.JENVMAN.2016.04.005

Kang, L.-S., & Cleasby, J. L. (1995). Temperature Effects on Flocculation Kinetics Using Fe(III) Coagulant. Journal of Environmental Engineering, 121(12), 893–901. https://doi.org/10.1061/(ASCE)0733-9372(1995)121:12(893)

Kinsner, W. (2005). A unified approach to fractal dimensions. International Conference on Computing and Information, 1(4), 26–46. https://doi.org/10.4018/JCINI.2007100103

Konduri, M. K. R., & Fatehi, P. (2017). Influence of pH and ionic strength on flocculation of clay suspensions with cationic xylan copolymer. Colloids and Surfaces A: Physicochemical and Engineering Aspects, 530, 20–32. https://doi.org/10.1016/J.COLSURFA.2017.07.045

Kozminykh, P., Heistad, A., Ratnaweera, H. C., & Todt, D. (2016). Impact of organic polyelectrolytes on coagulation of source-separated black water. Environmental Technology, 37(14), 1723–1732. https://doi.org/10.1080/09593330.2015.1130175

Lee, C. S., Robinson, J., & Chong, M. F. (2014). A review on application of flocculants in wastewater treatment. Process Safety and Environmental Protection, 92(6), 489–508. https://doi.org/10.1016/J.PSEP.2014.04.010

Li, D. H., & Ganczarczyk, J. (1989a). Fractal Geometry of Particle Aggregates Generated in Water and Wastewater Treatment Processes. Environmental Science and Technology, 23(11), 1385–1389. https://doi.org/10.1021/ES00069A009/ASSET/ES00069A009.FP.PNG_V03

Li, D. H., & Ganczarczyk, J. (1989b). Fractal Geometry of Particle Aggregates Generated in Water and Wastewater Treatment Processes. Environmental Science and Technology, 23(11), 1385–1389. https://doi.org/10.1021/ES00069A009/ASSET/ES00069A009.FP.PNG_V03

Li, W., Wang, J., Xin, H., Li, T., Duan, J., & Mulcahy, D. (2022). Determination of cost-effective optimum coagulant dosage for removal of disinfection by-product precursors in water treatment based on the theory of elasticity. Journal of Water Process Engineering, 47, 102782. https://doi.org/10.1016/J.JWPE.2022.102782

Lin, S., Kim, J., Hua, C., Park, M. H., & Kang, S. (2023). Coagulant dosage determination using deep learning-based graph attention multivariate time series forecasting model. Water Research, 232, 119665. https://doi.org/10.1016/J.WATRES.2023.119665

Liu, D., Li, F., & Zhang, B. (2009). Removal of algal blooms in freshwater using magnetic polymer. Water Science and Technology, 59(6), 1085–1091. https://doi.org/10.2166/WST.2009.046

Liu, P., Wang, J., Sangaiah, A. K., Xie, Y., & Yin, X. (2019). Analysis and Prediction of Water Quality Using LSTM Deep Neural Networks in IoT Environment. Sustainability 2019, Vol. 11, Page 2058, 11(7), 2058. https://doi.org/10.3390/SU11072058

Liu, W., & Ratnaweera, H. (2016). Improvement of multi-parameter-based feed-forward coagulant dosing control systems with feed-back functionalities. Water Science and Technology : A Journal of the International Association on Water Pollution Research, 74(2), 491–499. https://doi.org/10.2166/WST.2016.180

Luk, G. (1999). Removal Of Phosphorus By Metallic Coagulation: An Experimental Aid To Dose Computations. https://doi.org/10.2495/CMEM990541

Maćczak, P., Kaczmarek, H., & Ziegler-Borowska, M. (2020). Recent Achievements in Polymer Bio-Based Flocculants for Water Treatment. Materials 2020, Vol. 13, Page 3951, 13(18), 3951. https://doi.org/10.3390/MA13183951

Mackenzie, K., & Jemmett, A. E. (1971). Polymer shear stability. Wear, 17(5–6), 389–398. https://doi.org/10.1016/0043-1648(71)90045-7

Malcolm J. Brandt, K. M. J. A. J. E. D. D. R. (2016). Twort's Water Supply - Malcolm J. Brandt, K. Michael Johnson, Andrew J. Elphinston, Don D. Ratnayaka - Google Books. https://books.google.ca/books/about/Twort_s_Water_Supply.html?id=uk8mCAAAQBAJ&redir_esc=y

Manamperuma, L. D., Ratnaweera, H. C., & Martsul, A. (2016). Mechanisms during suspended solids and phosphate concentration variations in wastewater coagulation process. Environmental Technology (United Kingdom), 37(19), 2405–2413. https://doi.org/10.1080/09593330.2016.1150354

Manamperuma, L., Wei, L., & Ratnaweera, H. (2017). Multi-parameter based coagulant dosing control. Water Science and Technology, 75(9), 2157–2162. https://doi.org/10.2166/WST.2017.058

Mandelbrot, B. (1967). How Long Is the Coast of Britain? Statistical Self-Similarity and Fractional Dimension. Science, 156(3775), 636–638. https://doi.org/10.1126/SCIENCE.156.3775.636

Mandelbrot, B. B., & Wheeler, J. A. (1983). The Fractal Geometry of Nature. American Journal of Physics, 51(3), 286–287. https://doi.org/10.1119/1.13295

Manning, A. J., Baugh, J. V., Spearman, J. R., & Whitehouse, R. J. S. (2010). Flocculation settling Characteristics of mud: Sand mixtures. Ocean Dynamics, 60(2), 237–253. https://doi.org/10.1007/S10236-009-0251-0/METRICS

Matilainen, A., Vepsäläinen, M., & Sillanpää, M. (2010). Natural organic matter removal by coagulation during drinking water treatment: A review. Advances in Colloid and Interface Science, 159(2), 189–197. https://doi.org/10.1016/J.CIS.2010.06.007

Mensah-Akutteh, H., Buamah, R., Wiafe, S., & Nyarko, K. B. (2022). Optimizing coagulation–flocculation processes with aluminium coagulation using response surface methods. Applied Water Science, 12(8), 1–13. https://doi.org/10.1007/S13201-022-01708-1/TABLES/9

Molina, M. A., Pérez, C. A. A., & Leiva, C. A. (2020). Characterization of Filamentous Flocs to Predict Sedimentation Parameters Using Image Analysis. Journal of Sensors, 2020. https://doi.org/10.1155/2020/5248509

Nan, J., He, W., Song, J., & Song, X. (2009). Fractal growth characteristics of flocs in flocculation process in water treatment. 2009 International Conference on Energy and Environment Technology, ICEET 2009, 2, 582–588. https://doi.org/10.1109/ICEET.2009.379

Neis, U., & Tiehm, A. (1997). Particle size analysis in primary and secondary waste water effluents. Water Science and Technology, 36(4), 151–158. https://doi.org/10.1016/S0273-1223(97)00434-4

Niu, G., Yi, X., Chen, C., Li, X., Han, D., Yan, B., Huang, M., & Ying, G. (2020). A novel effluent quality predicting model based on genetic-deep belief network algorithm for cleaner production in a full-scale paper-making wastewater treatment. Journal of Cleaner Production, 265, 121787. https://doi.org/10.1016/J.JCLEPRO.2020.121787

Nti, S. O., Buamah, R., & Atebiya, J. (2021). Polyaluminium chloride dosing effects on coagulation performance: case study, Barekese, Ghana. Water Practice and Technology, 16(4), 1215–1223. https://doi.org/10.2166/WPT.2021.069

Ødegaard H. (1985). Engineering aspects of flocculation. Chemical Water and Wastewater Treatment, 81–102.

Ødegaard, H., Fettig, J., & Ratnaweera, H. C. (1990). Coagulation with Prepolymerized Metal Salts. Chemical Water and Wastewater Treatment, 189–220. https://doi.org/10.1007/978-3-642-76093-8_14

Parker, D. S., Kaufman, W. J., & Jenkins, D. (1970). Characteristics of biological flocs in turbulent regimes | WorldCat.org. https://search.worldcat.org/title/characteristics-of-biological-flocs-in-turbulent-regimes/oclc/10709108

Radoiu, M. T., Martin, D. I., Calinescu, I., & Iovu, H. (2004). Preparation of polyelectrolytes for wastewater treatment. Journal of Hazardous Materials, 106(1), 27–37. https://doi.org/10.1016/j.jhazmat.2003.08.014

Raj, S., Singh, H., & Bhattacharya, J. (2023). Treatment of textile industry wastewater based on coagulation-flocculation aided sedimentation followed by adsorption: Process studies in an industrial ecology concept. Science of The Total Environment, 857, 159464. https://doi.org/10.1016/J.SCITOTENV.2022.159464

Ratnaweera, H. (1991). Influence of the degree of coagulant prepolymerization on wastewater coagulation mechanisms. (Doctoral dissertation). Norwegian Institute of Technology, Trondheim. Norwegian Institute of Technology.

Ratnaweera, H., & Fettig, J. (2015a). State of the Art of Online Monitoring and Control of the Coagulation Process. Water 2015, Vol. 7, Pages 6574-6597, 7(11), 6574–6597. https://doi.org/10.3390/W7116574

Ratnaweera, H., & Fettig, J. (2015b). State of the Art of Online Monitoring and Control of the Coagulation Process. Water, 7(11), 6574–6597. https://doi.org/10.3390/W7116574

Ratnaweera, H., Lei, L., & Lindholm, O. (2002). Simulation program for wastewater coagulation. Water Science and Technology, 46(4–5), 27–33. https://doi.org/10.2166/WST.2002.0543

Ratnaweera, H., Odegaard, H., & Fettig, J. (1992a). Coagulation with Prepolymerized Aluminium Salts and their Influence on Particle and Phosphate Removal. Water Science and Technology, 26(5–6), 1229–1237. https://doi.org/10.2166/WST.1992.0565

Ratnaweera, H., Odegaard, H., & Fettig, J. (1992b). Coagulation with Prepolymerized Aluminium Salts and their Influence on Particle and Phosphate Removal. Water Science and Technology, 26(5–6), 1229–1237. https://doi.org/10.2166/WST.1992.0565

Ratnaweera, H., Odegaard, H., & Fettig, J. (1992c). Coagulation with Prepolymerized Aluminium Salts and their Influence on Particle and Phosphate Removal. Water Science and Technology, 26(5–6), 1229–1237. https://doi.org/10.2166/WST.1992.0565

Ratnaweera, H., Smoczyński, L., Lewandowski, A., & Bielecka, M. (2005). EFFICIENT CONTROL OF COAGULANT DOSING IN WASTEWATER TREATMENT.

Ren, P., Nan, J., Zhang, X., & Zheng, K. (2017). Analysis of floc morphology in a continuous-flow flocculation and sedimentation reactor. Journal of Environmental Sciences, 52, 268–275. https://doi.org/10.1016/J.JES.2016.04.007

Rosińska, A., & Dąbrowska, L. (2021). Influence of type and dose of coagulants on effectiveness of PAH removal in coagulation water treatment. Water Science and Engineering, 14(3), 193–200. https://doi.org/10.1016/J.WSE.2021.08.004

Sahu, O., & Chaudhari, P. (2013). Review on Chemical treatment of Industrial Waste Water. Journal of Applied Sciences and Environmental Management, 17(2). https://doi.org/10.4314/JASEM.V17I2.8

Saritha, V., Srinivas, N., & Srikanth Vuppala, N. V. (2017). Analysis and optimization of coagulation and flocculation process. Applied Water Science, 7(1), 451–460. https://doi.org/10.1007/s13201-014-0262-y

Shouci Lu, Robert J. Pugh, & Eric Forssberg. (2005). Chapter 7 Flocculation with polymers. Studies in Interface Science, 20(C), 354–414. https://doi.org/10.1016/S1383-7303(05)80008-0

Somasundaran, P., Das, K. K., & Yu, X. (1996). Current Opinions in Colloid and Interface Sciences. Current Opinion in Colloid & Interface Science, 1(4), 530–534. https://doi.org/10.1016/S1359-0294(96)80123-3

Surface Water: Phosphates and Other Waterborne Fertilizers. (n.d.). Retrieved March 6, 2024, from https://www.knowyourh2o.com/outdoor-4/phosphates-in-the-environment

Szabó, A., Takács, I., Murthy, S., Daigger, G. T., Licskó, I., & Smith, S. (2008). Significance of design and operational variables in chemical phosphorus removal. Water Environment Research : A Research Publication of the Water Environment Federation, 80(5), 407–416. https://doi.org/10.2175/106143008X268498

Tambo, N., & Watanabe, Y. (1979). Physical aspect of flocculation process—I: Fundamental treatise. Water Research, 13(5), 429–439. https://doi.org/10.1016/0043-1354(79)90035-6

Teng, T. T., San Wong, S., & Wei Low, L. (2014). Coagulation–Flocculation Method for the Treatment of Pulp and Paper Mill Wastewater. The Role of Colloidal Systems in Environmental Protection, 239–259. https://doi.org/10.1016/B978-0-444-63283-8.00010-7

Trinh, T. K., & Kang, L. S. (2011). Response surface methodological approach to optimize the coagulation–flocculation process in drinking water treatment. Chemical Engineering Research and Design, 89(7), 1126–1135. https://doi.org/10.1016/J.CHERD.2010.12.004

Vahedi, A., & Gorczyca, B. (2012). Predicting the settling velocity of flocs formed in water treatment using multiple fractal dimensions. Water Research, 46(13), 4188–4194. https://doi.org/10.1016/J.WATRES.2012.04.031

Vahedi, A., & Gorczyca, B. (2014). Settling velocities of multifractal flocs formed in chemical coagulation process. Water Research, 53, 322–328. https://doi.org/10.1016/J.WATRES.2014.01.008

Van Benschoten, J. E., & Edzwald, J. K. (1990). Chemical aspects of coagulation using aluminum salts—I. Hydrolytic reactions of alum and polyaluminum chloride. Water Research, 24(12), 1519–1526. https://doi.org/10.1016/0043-1354(90)90086-L

Wang, J. P., Chen, Y. Z., Wang, Y., Yuan, S. J., & Yu, H. Q. (2011). Optimization of the coagulation-flocculation process for pulp mill wastewater treatment using a combination of uniform design and response surface methodology. Water Research, 45(17), 5633–5640. https://doi.org/10.1016/J.WATRES.2011.08.023

Xiao, F., Huang, J. C. H., Zhang, B. jie, & Cui, C. wei. (2009). Effects of low temperature on coagulation kinetics and floc surface morphology using alum. Desalination, 237(1–3), 201–213. https://doi.org/10.1016/J.DESAL.2007.12.033

Xiao, F., Lam, K. M., Li, X. Y., Zhong, R. S., & Zhang, X. H. (2011). PIV characterisation of flocculation dynamics and floc structure in water treatment. Colloids and Surfaces A: Physicochemical and Engineering Aspects, 379(1–3), 27–35. https://doi.org/10.1016/J.COLSURFA.2010.11.053

Yang, Y., Zhao, Y. Q., Babatunde, A. O., Wang, L., Ren, Y. X., & Han, Y. (2006). Characteristics and mechanisms of phosphate adsorption on dewatered alum sludge. Separation and Purification Technology, 51(2), 193–200. https://doi.org/10.1016/J.SEPPUR.2006.01.013

Yao, M., Nan, J., & Chen, T. (2014). Effect of particle size distribution on turbidity under various water quality levels during flocculation processes. Desalination, 354, 116–124. https://doi.org/10.1016/J.DESAL.2014.09.029

Yaqub, M., Asif, H., Kim, S., & Lee, W. (2020). Modeling of a full-scale sewage treatment plant to predict the nutrient removal efficiency using a long short-term memory (LSTM) neural network. Journal of Water Process Engineering, 37, 101388. https://doi.org/10.1016/J.JWPE.2020.101388

Yateh, M., Lartey-Young, G., Li, F., Li, M., & Tang, Y. (2023). Application of Response Surface Methodology to Optimize Coagulation Treatment Process of Urban Drinking Water Using Polyaluminium Chloride. Water (Switzerland), 15(5), 853. https://doi.org/10.3390/W15050853/S1

Zarei Mahmudabadi, T., Ebrahimi, A. A., Eslami, H., Mokhtari, M., Salmani, M. H., Ghaneian, M. T., Mohamadzadeh, M., & Pakdaman, M. (2018). Optimization and economic evaluation of modified coagulation–flocculation process for enhanced treatment of ceramic-tile industry wastewater. AMB Express, 8(1). https://doi.org/10.1186/S13568-018-0702-4

Zhang, H., & Luo, D. (2004). Application of an expert system using neural network to control the coagulant dosing in water treatment plant. Journal of Control Theory and Applications, 2(1), 89–92. https://doi.org/10.1007/S11768-004-0030-X

Zhao, C., Zhou, J., Yan, Y., Yang, L., Xing, G., Li, H., Wu, P., Wang, M., & Zheng, H. (2021). Application of coagulation/flocculation in oily wastewater treatment: A review. Science of The Total Environment, 765, 142795. https://doi.org/10.1016/J.SCITOTENV.2020.142795

Zheng, H., Zhu, G., Jiang, S., Tshukudu, T., Xiang, X., Zhang, P., & He, Q. (2011). Investigations of coagulation–flocculation process by performance optimization, model prediction and fractal structure of flocs. Desalination, 269(1–3), 148–156. https://doi.org/10.1016/J.DESAL.2010.10.054

Zhong, R., Zhang, X., Xiao, F., Li, X., & Cai, Z. (2011). Effects of humic acid on physical and hydrodynamic properties of kaolin flocs by particle image velocimetry. Water Research, 45(13), 3981–3990. https://doi.org/10.1016/J.WATRES.2011.05.006

Zhou, Y., & Franks, G. V. (2006). Flocculation Mechanism Induced by Cationic Polymers Investigated by Light Scattering.

Zouboulis, A., Tzoupanos, N., & Moussas, P. (2007). (PDF) Inorganic pre-polymerized coagulants: Current status and future trends. https://www.researchgate.net/publication/228628710_Inorganic_pre-polymerized_coagulants_Current_status_and_future_trends